Published in final edited form as:
Methods Mol Biol. 2010 ; 627: 15–54. doi:10.1007/978-1-60761-670-2_2.

The Role of Mass Transport Limitation and Surface Heterogeneity in the Biophysical Characterization of Macromolecular Binding Processes by SPR Biosensing

Peter Schuck and **Huaying Zhao**
Dynamics of Macromolecular Assembly, Laboratory of Bioengineering and Physical Science, NIBIB, NIH, Bethesda MD 20892, U.S.A

Abstract

This chapter presents an introduction to the kinetic analysis of SPR biosensor data for the determination of affinity and kinetic rate constants of biomolecular interactions between an immobilized and a soluble binding partner. The need to be aware of and critically tests the assumptions underlying the analysis models is emphasized and the consequences for the experimental design are discussed. The two most common sources of deviation in SPR surface binding kinetics from the ideal pseudo-first order binding kinetics of bimolecular reactions are mass transport limitations and the heterogeneity of the surface sites. These problems are intrinsic to the use of a biosensor surface for characterizing interactions. The effect of these factors on the observed binding kinetics, and strategies to account for them are reviewed, both in the context of mathematical data analysis, as well as the design of the experiments and controls.

Keywords

binding kinetics; affinity distribution; thermodynamics; mass transport limitation; surface binding; optical biosensor; Tikhonov regularization

1. Introduction

Since the introduction of SPR biosensing in the early 1990s as a biophysical technique for studying molecular interactions, it has gained great popularity and has been used very successfully in a broad range of applications (1–5). The methodology has undergone a significant evolution, especially with regard to our understanding of the physical processes taking place at the sensor surface and in the immobilization matrix. Despite the numerous pitfalls that were encountered and exhaustively explored when SPR biosensors were first commercially introduced, many sophisticated SRP studies in the literature since then have established that SPR technology can be used as a reliable biophysical research tool, if carefully controlled.

The use of optical biosensors for the characterization of macromolecular interactions has specific advantages that can be unique and very powerful when applied to a suitable system.

First, by adjusting the number of immobilized surface sites the binding signal can be chosen independent of the affinity of the interaction. This is in contrast to solution methods, which, in order to ensure the population of all binding partners both free and in complex, have to be conducted at very low concentrations for high-affinity systems. The SPR signal relies on refractive index changes in the evanescent field at the surface, and because the refractive index increment of biomacromolecules is typically small, relatively high surface concentrations of the immobilized binding partner are required to achieve good signal/noise levels. However, because the surface concentration is (ideally) not imposing constraints on the type or strength of interaction that is to be studied, the label-free study of high-affinity interactions is possible.

Second, the configuration of one binding partner immobilized in the detection volume, and a second binding partner (the ‘analyte’) initially being essentially undetected in the bulk solution but becoming visible when bound to the surface, allows the real-time observation of the progress of complex formation. If a precise, timed control of the bulk analyte concentration is possible in the SPR instrument, such as provided for by an efficient flow system or a well-stirred cuvette system, the quantitative interpretation of the kinetics of the binding progress is possible. Besides the potential for measuring kinetic rate constants, this may allow estimating equilibrium constants for very slowly equilibrating systems without reaching equilibrium.

Third, the biosensor surface is essentially a miniaturized affinity chromatography purification system. This has several advantages. It opens the possibility for a wide variety of configurations for studying multi-protein complexes, a topic of increasing interest (6). Also, at least for small analytes, the elution of material from the SPR surface lends itself to mass spectrometric identification (7–11) (see also Chapters Roepstorff, Nedelkof). Finally, the binding experiment is tolerant to non-reacting contaminants in the sample preparations.

For these features to be exploited, some difficulties inherent to biosensing must be overcome. Obviously, there is the need for one binding partner to be stably attached to the surface. This raises questions regarding the best strategy of attachment such that the binding epitopes are presented in their native state with unimpeded access for the soluble analyte. This is not trivial, and goes beyond the question of the choice of immobilization chemistry; we have to consider the influence of the whole sensor surface on the immobilized macromolecule. In fact, as will be outlined below, we should expect in most cases an ensemble of surface sites with a spectrum of binding properties to arise from immobilization. In addition to artifactual low-affinity sites resulting from partial protein degradation, this can also include microheterogeneity. Similarly, the surface itself can present low-affinity ‘non-specific’ binding sites for the analyte even in the absence of the immobilized binding partner. Further, for some interacting bimolecular systems the surface itself may constitute a third component promoting or suppressing the complex formation.

Another fundamental problem introduced by the physical separation of immobilized sites at the surface and the analyte in the bulk solution is the need to establish efficient mass transfer between the bulk and the surface. Otherwise the analyte concentration near the surface will be different from the bulk concentration, exhibiting either a local depletion zone or retention

zone, respectively (dependent on the phase of the experiment), and characteristic deviations in the binding progress ensue. For understanding the importance of this effect it is crucial to appreciate that binding and diffusion are coupled phenomena on two levels. Macroscopically, the more surface sites there are, the more effective the mass transport needs to be in order to replenish the analyte drawn to the surface. Microscopically, analyte molecules can only diffuse while they are not bound, and therefore the effective diffusion through an array of surface sites proceeds slower than the diffusion in the bulk. This difference can be many orders of magnitude, dependent again on the density and binding parameters of the surface sites. Therefore, despite the deceptively short distances across the sensor surface, analyte concentration gradients may exist and mass transport may be associated with long-lived moving front phenomena (12, 13). The presence of low-affinity 'non-specific' surface sites, even if non-specific and clearly distinct from the sites of interest will therefore impact the mass transfer.

Thus, in order to interpret the observed time-course of the binding signal as if it directly reflects the properties of the interacting molecules of interest, rather than the physical properties of the particular surface/flow configuration, or just an average of an ensemble of proteins with a range of surface-induced conformations, we need to probe the true physical binding process taking place. This can be a challenging proposition since we do not have microscopic knowledge of the surface site distribution and the local parameters of the physical environment, and can only infer indirectly the nature of the process we observe from the evolution of a single signal. It is crucial to keep in mind this fundamental problem in SPR biosensing. Unfortunately, the history of SPR kinetic analysis exposes a long series of silent or explicit assumptions about key aspects of the observed binding process which were implemented in various analysis approaches, but turned out to be convenient, yet invalid simplifications. Therefore, one achieving a correct and reliable interpretation of the data requires the art of recognizing the silent (or occasionally explicit) assumptions underlying the different analysis ideas, and to critically question and experimentally test them whenever possible.

A variety of experimental design tools are available, and methods for the stringent comparison of the measured data with the predictions from different models. This chapter is not meant to be a formal review, but rather an introduction to highlight experimental limitations intrinsic to optical biosensing fundamentally arising both from the need of mass transport to the sensor surface and from the immobilization of a binding partner to the surface. We discuss strategies how to detect these problems and to experimentally minimize their influence on the estimation of the molecular interaction parameters of interest. We recapitulate robust and realistic approaches to account for their influence in the data analysis, as well as the limitations of the analytical descriptions. Accordingly, the chapter is structured in three main sections. We start with the 'ideal pseudo-first order binding', establishing some of its characteristic features and requirements for a sensible analysis of such binding data. Next, mass transport limited surface binding processes are examined in detail, followed by the description of surface heterogeneity, and a discussion of the relationship between these sources or artifacts. Finally, we draw conclusions for experimental and data analysis strategy.

2. The First Goal – Establishing Ideal Pseudo-First Order Binding Kinetics (or How the Data Deviate From This Model)

2.1. Basic Features of Ideal Surface Binding

It is non-trivial to ascertain that binding is taking place with ideal pseudo-first order binding kinetics. In this paragraph, we will discuss criteria that should be applied to probe the data for their consistency with this model. From the experience with data collected in our own laboratory as well as from the examination of the literature, we find that, in fact, it is rarely observed (2, 14, 15). Nevertheless, this process serves as a methodological reference point as it represents the simplest bimolecular surface-binding reaction. Therefore, it is important to establish its hallmarks and the requirements for its rigorous analysis. Further, it can be quite informative to discern the specific features of the data that deviate from the pseudo-first order predictions. This will help to diagnose the process that most likely takes place at the surface.

The pseudo-first order kinetics describes the surface-binding process where we have a concentration of free analyte, *c*, held constant either by replenishing the surface-bound molecules through the flow across the surface, or because of the negligible number of surface-bound molecules relative to the total number of analyte molecules in the reservoir above. The binding progress *s(t)* then follows the rate equation

$$\frac{ds}{dt} = k_{on} c (s_{\max} - s) - k_{off} s \quad (1)$$

, the first term accounting for the binding reaction to previously unoccupied surface sites (a subset of the total number of surface sites s_{max}) with the rate constant k_{on}, and the second term accounting for the continuous dissociation of analyte with the rate constant k_{off} due to the finite life-time of the complex ($t = k_{off}^{-1}$). As the binding proceeds and the surface sites fill up, the dissociation term becomes increasingly more important, until it matches the association term and an equilibrium or steady-state is attained. The overall time-course is a single-exponential approach of a steady-state signal. If we apply the analyte starting at the time t_o for a total contact time t_c, we can integrate the rate equation and obtain the binding progress in the association phase

$$s_a(c,t) = s_{eq}(c) \left(1 - e^{-(k_{on} c + k_{off})(t - t_0)}\right) \quad (2)$$

, asymptotically approaching the steady-state response

$$s_{eq}(c) = \frac{s_{\max}}{1 + (K_A c)^{-1}} \quad (3)$$

which depends only on the equilibrium constant $K_A = k_{on}/k_{off}$ (or $K_D = k_{off}/k_{on}$) (16). After the analyte is removed, we see only the dissociation of bound analyte from the surface sites, which causes a single-exponential decay of the signal

$$s_d(c,t)=s_a(c,t_c)e^{-k_{off}(t-t_c)} \quad (4)$$

An example for the shape of the kinetic binding signal *s(c,t)* and the equilibrium isotherm $s_{eq}(c)$ at different concentrations is given in Figure 1.

2.2. Least-Squares Fitting the Pseudo-First Order Reaction Model to Experimental Data

This model should be fit globally to the data acquired at different analyte concentrations or flow-cells, to test whether or not it is consistent with the data. For this test to be meaningful, all data points (that are free of experimental artifacts) must be included, but also the experiment must be carried out such that the experimental data actually contain the required information.

Obviously, the most important parameter is the signal-to-noise ratio, which we recommend to be at least on the order of ~ 100. For much smaller signals, such as those proposed in (17), the data may be fit with certain models (possibly even generating acceptable statistical error intervals for the question under study) but the validity of the models cannot be tested with confidence, as shown in (18, 19). In the extreme case, any model will fit reasonably well to data that have amplitudes not much higher than the noise.

Regarding the quality of fit, there has been some uncertainty in the SPR field about what constitutes an acceptable fit. This is not unexpected for a new technique, since we have to make some allowance for unavoidable systematic errors, such as baseline drifts, injection artifacts from buffer changes, temperature and pressure fluctuations, and only experimental experience allows us to make these unavoidable judgments. However, experimental SPR technology has matured, and it has become clear that SPR data are usually highly reproducible, and one should apply the same stringent requirements as is custom in most other biophysical disciplines: When looking at the residuals (i.e. the difference between the fit and the data), they should be distributed uniformly and have a magnitude on the order of the noise of the data acquisition. We have shown recently that after accounting for surface site heterogeneity, kinetic SPR data can in fact usually be modeled to that level of detail (see below). An example is shown in Figure 2.

If the model doesn’t fit, especially if the deviations appear non-random, we have to conclude that the model used does not correctly capture the process observed in the experiment. From common sense, it seems that very small deviations would affect mostly the details of the analysis and perhaps widen the error intervals or slightly bias the parameter estimates, whereas substantial deviations should be expected to render the derived ‘best-fit’ parameters entirely meaningless. Unfortunately, this judgment is not rigorous, and difficult to justify mathematically or statistically.

2.3. Qualitative Features of Pseudo-First Order Binding Kinetics and Consequences for Conducting Experiments

There are qualitative requirements the data must fulfill in order to satisfy convincingly the test for pseudo-first order binding (and to allow a global fit with the pseudo-first order binding model). These are related to certain characteristic features of pseudo-first order

binding kinetics, some of which can be tested quite easily even by visual inspection or back-of-the-envelope calculations (20). They may help us gain confidence in the overall interpretation.

First, both the association and the dissociation process are single exponentials. Apparent multi-exponential behavior in both is an unequivocal sign of more complex binding reactions involving multiple sites or multiple states, or of mass transport limitation (see below). In order to establish that the data are single-exponential and to enable us measuring the exponent (i.e. the rate constants), it is essential that the data exhibit curvature. Generally, one could say that it is the curvature in the data that contains most information for the analysis with most models. For an exponential process to be well defined, the observation time should be on the order of several-fold the characteristic decay time (or life-time) t, which is here $t = (k_{on}c + k_{off})^{-1}$ for the association phase and $t = k_{off}^{-1}$ for the dissociation phase. This may not always be possible in practice, especially for slowly dissociating complexes. However, this should be kept in mind as a goal in the experimental design, and as a caveat in the data interpretation of shorter experiments. Truncations of the data set beyond the regions of artifacts from buffer changes are destroying information and should be avoided. An example for how a poorly designed, arbitrarily truncated data acquisition time can lead to a mis-interpreted binding process is shown in Figure 3.

As can be recognized from Equation (2), the association attains steady-state with a rate constant that dependent on concentration, following $k_{obs}(c) = k_{on}c + k_{off}$. Consistency with this linear concentration behavior will be apparent in the global least-squares fit of the data. Linearization of the equation (2) and separate analysis of $k_{obs}(c)$ and k_{off} can lead to significant errors and frequently rather arbitrary results (in particular when combined with short data acquisition or data truncation). Since the association proceeds to steady-state more slowly at lower concentrations, it is advisable to extend the experimental contact time for the association/dissociation cycles with these concentrations (Figure 1). This not only improves the kinetic information content of the lower concentration data, but also allows to better determine the steady-state response (see below).

The dissociation phase is characterized by a single dissociation rate constant, independent of the analyte concentration that was applied in the preceding association phase. This is due to the fact that the binding sites and complexes have no memory of their history. Therefore, the overlay of the dissociation traces, when adjusted for baseline offsets and aligned at the start of the dissociation phase, should lead to curves that do not intersect. For the same reason, experiments conducted at different contact times for the analyte during the association phase should be followed by dissociation phases exhibiting the same dissociation rate, independent of contact time.

Finally, the steady-state values that are asymptotically attained at long association times, to the extent that they can be estimated from the experimental data, should follow an isotherm as indicated in Figure1B. Half-saturation is obtained at $c = K_D$, and 10% and 90% saturation at 0.1-fold and 10-fold K_D, respectively, and naturally, the K_D estimate from this isotherm should be identical to the ratio of k_{off}/k_{on} from the analysis of the binding kinetics. These are

checks for self-consistency which frequently can be applied quickly (20). Again, a global least-squares fit will constrain the model to be internally consistent.

For both the binding isotherm analysis as well as the analysis of the binding kinetics, it is highly desirable that a range of analyte concentrations be used, starting from well below K_D up to 10-fold K_D. Clearly, if the concentration range that produces saturation of the surface sites is not accessed experimentally, the estimated saturation signal will be correlated with the K_D estimate in the data analysis. Further, at concentrations below K_D, many kinetic processes other than pseudo-first order binding will exhibit traces very similar to the expected single-exponential asymptotic attainment of a steady-state, and the incorporation of higher concentration data will enable better discrimination of the binding process. If the steady-state binding data cover a wide enough concentration range, the equilibrium constant may be determined without reference to the binding kinetics, which may be helpful if no simple model explaining the binding kinetics can be found. Experiments at a single concentration will neither reveal good estimates of kinetic rate or equilibrium constants, nor allow conclusions on the type of binding process observed, nor allow us to diagnose the presence of artifacts.

Many of the historic methods proposed when SPR technology was first introduced to the study of macromolecular interactions did not require or were in conflict with some of the above criteria. Nevertheless they generally implied *a priori* assumptions that the binding process is a pseudo-first order reaction. However, with the overwhelming evidence accumulating that most experimental SPR kinetic data do actually not follow this model, the need has become obvious to demonstrate that the binding model actually applies. Only in this case can one verify that the numbers obtained are meaningful in that they really reflect molecular parameters of interest. On the other hand, if the data are collected and analyzed according to these criteria, this will not only help establishing that a simple first-order binding kinetics takes place, but also help for the characterization of binding process that are more complicated.

Alternative experimental configurations have been proposed, including the continuous accumulation of bound material obtained in a step-wise increased analyte concentration, followed by only a single dissociation phase (Figure 1A inset). This idea was first introduced by us in the context of equilibrium titration with circulating sample (21). One obvious advantage is that of saving time (since no dissociation in between the application of different analyte concentration, and due to the slightly shorter association phases needed during the application of each but the first concentration). In the conventional linear flow configuration, the total analyte amounts required can be reduced slightly, although the saving can be more substantial in the configuration with circulating (21) or oscillating sample (22). The biggest practically advantage in most cases is certainly the absence of a surface regeneration step in between the association phases.

A disadvantage of this configuration is the loss of information in the association kinetics: It is easy to see that with small concentration increments, the approach to the new steady-state level will be close to exponential even in highly mass transport limited cases. In contrast, in the conventional configuration of multiple association/dissociation cycles, the application of

concentrations greater than K_D can exhibit the linear initial association kinetics so characteristic for mass transport limited binding (see below). The dissociation phase, unfortunately, is not as discriminatory, since in mass transport limited cases it will resemble a double-exponential, which could be caused by many processes. The loss of information will be compounded when the individual steps do not lead to close attainment of steady-state, as in the variation of the titration method proposed by Karlsson and co-workers (23). In this case characteristic information on the nature of the association phase kinetics as well as on the equilibrium constants may be destroyed by the experimental design.

2.4. Deviations from the Pseudo-First Order Model

As mentioned above, it is rare that the SPR surface binding data of protein-protein interactions actually meet the criteria for pseudo-first order binding. The most commonly observed deviation from the ideal pseudo-first order binding includes a slow signal increase in what should ideally be a steady-state signal at high analyte concentrations. This can arise, for example, from heterogeneity of the surface sites or heterogeneity of the analyte. Another widespread feature is the lack of saturation of the steady-state response as a function of concentration, which points to the existence of weaker, possibly non-specific binding sites. Finally, partially linear association signals are frequently observed, a signature of mass transport limitation.

Some experimental factors can introduce systematic errors, such as baseline drifts and the need to subtract signals from bulk effects measured on reference surfaces (24, 25). The magnitude of these effects needs to be experimentally assessed for the surface under study in the reaction conditions, and the experimental design and the data to be analyzed should be chosen such as to minimize these effects.

Before proceeding to review methods to address surface site heterogeneity and mass transport limited binding, we also have to assume in the following that we can rule out multi-valent surface attachment of analyte. Multi-valent surface attachment could be caused, for example, by small populations of analyte oligomers, or by the presence of more than one binding epitope on the analyte molecule capable of binding simultaneously to the immobilized binding partner at the surface. In these cases, a fraction of surface bound molecules may undergo a second binding event with a nearby binding site. This subpopulation will experience a dramatically different dissociation kinetics, since now both attachments have to be severed simultaneously in order for the analyte to become free. In many cases, this makes the binding virtually irreversible on the time-scale of the experiment, and consequently this analyte fraction will continuously accumulate at the surface and may be substantially over-represented among the surface-bound analyte relative to its abundance in the bulk analyte flow. Unfortunately, since there is no knowledge of the distribution of surface sites and their local mobility in the immobilization matrix, which would govern the likelihood for multivalent attachment, it is impossible to realistically interpret such binding kinetics (26, 27). (Although one can write more or less sophisticated binding equations, they have to rely on detailed knowledge of the physical properties of the surface and the immobilization matrix, requiring parameters that are not known at all, or not with any

degree of confidence. Alternatively, they are so oversimplified to be yield in our opinion essentially meaningless best-fit parameters.)

In principle, multi-valent surface attachment can be minimized experimentally, for example, by chromatographic removal of the analyte oligomers that are present at least in trace amounts in many or even most protein preparations (28–30), and/or by verify analytically the absence of oligomers by sedimentation velocity analytical ultracentrifugation (31). More difficult are cases where the analyte exhibits reversible self-association, either free in solution, or promoted by the high local macromolecular concentration inside the immobilization matrix (if used). If there is any known tendency for the analyte to exhibit such oligomerization, it cannot be used in quantitative kinetic SPR experiments as the mobile binding partner, and the role of mobile and immobilized binding partner should be reversed. If both binding partners exhibit the potential for multimerization, SPR surface binding cannot be used to assess quantitatively the molecular binding parameters, and instead solution binding assays are required (see Note 1).

If the above criteria for data collection have been fulfilled, fortunately, the binding of (partially) multivalent analyte should not be correlated much with the binding kinetics to multiple independent surface sites, and with mass transport limited binding. The unrecognized presence of multi-valent analyte will degrade the quality of fit with the latter models, or *vice versa*, an excellent fit with the surface heterogeneity and/or mass transport limited model (to suitable data sets) suggests the absence of multi-valent analyte.

If the kinetic surface binding data deviate from the pseudo-first order binding, which is the case in the overwhelming majority of protein-protein interactions encountered in our laboratory and in the literature, one possible way to proceed is the postulation of more complex chemical interaction schemes, such as conformational change or multi-site models. We believe that most experimental data sets that have a concentration-dependent, monotonically increasing signal in the association phase and a monotonically decreasing signal in the dissociation phase can be force-fitted with one or more sufficiently complex reaction schemes (32), simply because the shape of the experimental binding progress curves is not very rich in information. However, whether or not these models reflect correct process taking place cannot be answered easily. Following the principle of Occam's razor – which recommends us to interpret the data with the simplest possible model – would lead us not to invoke complex reaction schemes, but to probe first whether common surface-induced artifacts can explain the shape of the data, and whether a model accounting for these effects can yield estimates for the binding parameters for pseudo-first order chemical reactions. Further confidence can be gained with the application of experimental tools that can establish qualitatively the key aspects of the model, such as the variation of the analyte contact time in the association phase, the variation of flow parameters, immobilization protocols, and different competition assays (33).

[1]It should be noted that this is true irrespective of the fact that the molecules under study may include surface receptors that in the biological environment exist and act at a surface. Unless this exact biological surface can be used, e.g., by coating the SPR surface with actual cell membranes, the differences of the native and the artificial environment in the SPR sensing volume with respect to the precise physical environment and the surface site distribution will be the dominating factor for the observed surface binding kinetics, yielding parameters potentially many orders of magnitude different from those in the native environment.

The surface-site heterogeneity and the mass transport limitation model will be described in the following with respect to their potential and limitation for estimating molecular binding parameters, and with their corresponding experimental tools.

3. The Influence of Mass Transport on the Binding Kinetics

3.1. Physical Picture

Mass transport limitation (MTL) is caused fundamentally by the analyte and the surface sites initially being located physically at different points. In any surface binding experiment, this brings about the necessity to transport the analyte to the surface in the association phase, and to transport it away from the surface in the dissociation phase. As we will see, MTL problems in the association and dissociation phase are of the same magnitude, even though they show in different ways. Under MTL conditions, in the association phase a depletion zone will be caused ($c_s < c_0$) where the local concentration is lower than the target in the bulk (Figure 4A), whereas in the dissociation phase a retention zone is present close to the surface sites ($c_s > 0$), that allows dissociated analyte molecules to rebind to empty surface sites before they can escape into the bulk flow (Figure 4B). These concentration gradients (relative from surface to bulk) diminish continuously with time as steady-state is attained. Unless the life-time of these gradients is much faster than the time-scale of the chemical kinetics, they will have profound influence on the observed binding kinetics.

One can distinguish MTL on different length scales, and each can be the rate limiting step causing MTL (2) (Figure 5). First, there is the macroscopic transport, which may be accomplished, for example, by a conventional pressure-driven flow system, a stirred cuvette system, a manual pipette-type probe, or other more sophisticated configurations, such as exploiting electro-osmotic flow (34). Since the pressure-driven laminar flow system is the most commonly employed, such a system will be assumed in the following. Our macroscopic experience suggests that in order to adjust the analyte concentration in the flow cell volume to a certain target concentration c_0, we should ensure that it be rinsed with at least several times its volume. As examined by (35, 36), this imposes minimal flow velocities for the observation of binding reactions with high k_{off}.

Second, we can consider the properties of the laminar flow across the surface. The ordinary non-slip boundary conditions will cause a non-stirred liquid layer through which the analyte must transport by diffusion (37). Laminar flow-assisted transport to a reacting surface has been well studied in hydrodynamics and chemical kinetics, and simple approximate expressions for the effective molecular transport rate dependent on the flow geometry and the molecular diffusion coefficient are available (38). Most importantly, they show that the transport rate constant changes with the cube root of the flow velocity, i.e., in order to double the transport rate through the stagnant layer an 8-fold increase in flow velocity is necessary.

Finally, the perhaps most intriguing transport step is the microscopic transport through the sensing volume itself. Most commonly, a hydrophilic polymer matrix is employed as immobilization support and for suppressing non-specific binding, often consisting of several hundred kDa carboxymethyl dextran randomly attached to the surface (39). The thickness of

such a matrix is estimated variously to be only on the order of 100 – 400 nm thick (40, 41). We have shown experimentally and theoretically that it also can be the rate-limiting step of transport, dependent on the surface properties and the properties of the interacting macromolecules (12). Key to the propagation of free analyte in the matrix is the recognition that it does not proceed with bulk diffusion coefficients, but instead has to be regarded as a coupled reaction/diffusion process (42). Mass transport limited binding and binding limited mass transport are two sides of the same physical phenomenon. Since analyte molecules can only diffuse during the time they are not bound to the surface sites (be it the specific sites of interest or other, perhaps non-specific sites) we can estimate the order of magnitude of an 'effective diffusion constant D_{eff}' that is the bulk diffusion constant D_0 reduced by a factor τ_{free}/τ_{bound} reflecting the time-average state the analyte is unbound. We can estimate the order of magnitude of this factor from the steady-state condition *via* the ergodic theorem, and approximate this factor as the ratio of the population average of free and bound c_{free}/c_{bound} analyte states in the matrix. Since typical SPR signals of 100×10^{-6} refractive index units (~ 100 RU) require on the order of ~ 1 mg/ml concentrations in a ~100 nm thick matrix, the number of surface sites in the detection volume is very high, for example ~100 μM of a 10 kDa protein. When studying high-affinity reactions with K_D < 10 nM, analyte molecules will spend most of the time in the bound state, and therefore the effective diffusion coefficient can be lowered easily by a factor 10^4, which brings the diffusion time through the detection volume from the fraction of a millisecond in free solution to in the order of seconds in the presence of surface sites. Any transient binding will delay diffusion, not only binding to specific sites; non-specific interactions can likewise significantly exacerbate this effect and further reduce diffusion (15) (see Note 2). Matrix mediated transient interactions should be strongly dependent on the macromolecules of interest, as well as pH and ionic strength of the buffer.

Further, besides the fundamental problem of diffusion through an array of sites, if a polymeric immobilization matrix is used, the physical properties of the matrix itself hamper the mobility of the analyte. There is partitioning of analyte into the matrix, which will reduce the concentrations and diffusion fluxes (although not the equilibrium response due to the proportionally higher analyte chemical activity), and restricted diffusion due to the presence of the carbohydrate chains and immobilized proteins (43). (It seems possible that under some circumstances the immobilization of proteins into the matrix by random chemistries may lead to its crosslinking.)

Because the detection volume extents quite some distance in transverse direction parallel to the flow, a problem of the surface binding reaction coupling to diffusion will exist in a similar form for a flat, truly two-dimensional surface, here reducing the effective transverse diffusion in the stagnant boundary layer. It has been shown that near a surface the basic hydrodynamics of macromolecular diffusion is altered, resulting in reduced mobility irrespective of the presence of a matrix (44).

[2]For example, if an analyte of 100 kDa at a concentration of 10 nM leads to a signal from non-specific binding on the level of 10-6 refractive index units (1 RU), which may be difficult to distinguish from a bulk shift, the ratio c_{free}/c_{bound} only considering the non-specific sites is 0.01, and this alone leads to an extra reduction of the analyte mobility by a factor 100.

As a consequence, when considering this microscopic step, we have to take into account the full three-dimensional distribution of the surface sites and the density distribution of the matrix, which is most certainly not uniform perpendicular to the surface (45) and also dependent on electrostatic and steric interactions (46) that may change with buffer conditions. Unfortunately, the complexity of the matrix and the level of detail needed on the distribution of the immobilized surface sites make an analytical model very difficult. However, this does not preclude us from making theoretical predictions for certain plausible parameters and to study the features of MTL for simplified model systems.

Given all the unknowns and their paramount influence on the extent of MTL, it is very difficult to predict *a priori* the chemical on-rate constants where MTL will become relevant. From practical experience, one should consider the possibility of MTL for reactions with k_{on} greater than 10^5/Msec, although even slower chemical kinetics may be mass transport limited under unfavorable conditions. One problem with this assessment is, however, that generally the chemical rate constants are not known independently, and obviously the apparent rate constant estimates obtained from the SPR biosensing themselves cannot be trusted since under MTL conditions they may be significantly too low (see below).

3.2. Effect on the Observed Binding Kinetics

At the most basic conceptual level, we can use a two-compartment model to account for the fact that there are different regions in space with different analyte concentrations, and that there can be transport between these regions (47). More specifically, we can postulate that there is a region ‘close to the surface’ with analyte concentration c_{surf} and the region ‘far from the surface’ where the analyte concentration is that of the bulk, and that the transport is governed by a rate constant k_{tr}. Binding then proceeds locally as indicated in Eq. (1), but at the surface analyte concentration c_{surf}. This leads to a combined rate equation for compartment-like transport and binding:

$$\begin{aligned}\frac{dc_{surf}}{dt} &= k_{tr}(c - c_{surf}) - \frac{ds}{dt} \\ \frac{ds}{dt} &= k_{on}c_{surf}(s_{\max} - s) - k_{off}s\end{aligned} \quad (5)$$

(see Note 3). It is important to realize that this model only provides a limited view of mass transport effects because each compartment is assumed to be instantaneously well-mixed (see below). However, the two-compartment model is useful as a first-order approximation, to the extent that we could in always ‘discretize’ an existing small concentration gradient into two homogeneous regions separated by a single concentration step (and analogously, n-compartment models could model the concentration gradients with (n-1) steps (13)).

This approximation allows us to predict some of the essential features of MTL. As illustrated in Figure 6, MTL causes both the association and the dissociation phase to exhibit

[3]In equation 5, we have chosen to express the transport rate constant k_{tr} in signal units of RU×M^{-1}×sec^{-1}. For the geometry of the Biacore instruments, typical numerical values are 10^7 to 10^{12}, and they are best thought of on a logarithmic scale. If a number of assumptions are made, among them the neglect of transport through the immobilization matrix, k_{tr} can be theoretically related to a macromolecular diffusion coefficient. However, in a careful study we have not obtained reasonable values for the diffusion coefficients with this approach in practice (13).

slower kinetics. In the association phase, the binding progress deviates from the exponential towards an initially more linear approach of steady-state. In contrast, the dissociation phase shows greater curvature at signals close to saturation, mimicking the existence of a fast phase and a slow phase. We emphasize that this is here not due to the presence of a second class of sites, but purely a consequence of mass transport limited binding. If the binding level is less than approximately half saturation, qualitatively only a slow phase seems to appear.

One a more quantitative level, the so-called 'steady-state approximation' yields further insights. Since the surface concentration will quickly assume a steady-state with dc_{surf}/dt being approximately zero (i.e., all material arriving in the surface compartment from bulk will be used up for new binding events), we can insert this in Eq. (5) and arrive at the picture of apparent rate constants

$$\frac{ds}{dt} = k_{on}^{(app)} c_0 (s_{\max} - s) - k_{off}^{(app)} s$$
$$\frac{k_{on}^{(app)}}{k_{on}} = \frac{k_{off}^{(app)}}{k_{off}} = \frac{1}{1 + \frac{[k_{on}(s_{\max} - s(t))]}{k_{tr}}} \quad (6)$$

Although Eq. (6) formally looks like the ideal rate equation (1), both rate constants are reduced by a factor that grows with k_{on} ($s_{\max}$ - $s(t)$)/k_{tr}, i.e. is dependent on the occupation of the surface sites and change with time. We can interpret k_{on} ($s_{\max}$ - $s(t)$)/k_{tr} as the probability of analyte binding to the empty surface sites relative to the probability of transport. In the dissociation phase, this can immediately be reconciled with the picture (Figure 4B) showing the retention of analyte close to the surface due to rebinding before the analyte can escape. Analogously, in the association phase the same factor describes the magnitude by which the surface sites themselves represent sinks for analyte preventing c_{surf} to be raised uniformly to the level of c_0. Thus, the magnitude of the effect of MTL on the apparent on-rate constant and the apparent off-rate constant is the same, although the effect on the shapes of the profiles is different (see Note 4). The compartment model can be extended to models with multiple compartments and multiple surface sites, and we have shown that under steady-state conditions, more general equations analogous to (6) can be derived.

We can see from (6) also that, under conditions of virtual saturation of all sites, the binding process evolves with rates close to the true chemical rate constants (see Note 5). This is consistent, again, with the picture introduced above of binding (to open sites) limiting the transport, therefore causing MTL or rather limited mass transport. On the other hand, for experimental configurations that include only concentrations lower than K_D, the fractional saturation will never exceed 50%, such that the ratio k_{on} ($s_{\max}$ - $s(t)$)/k_{tr} will not change during the course of the binding experiment by more than a factor of two (although the

[4]Because of the latter it is not possible to use an ideal model Eq. (1) to fit data that are mass transport limited, and expect the ratio of the apparent rate constants to reflect the true equilibrium constant. The least-squares fit will be poor, and biased differently in association and dissociation dependent on the experimental configuration, such as length of association and dissociation phases, and concentrations chosen.

[5]This should not be misunderstood to mean that the binding progress close to reaching steady-state is not mass transport influenced, as suggested by Karlsson et al. (57). It only vanishes close to saturation of all sites.

influence of MTL could be arbitrarily large). Therefore, the MTL binding processes takes on shapes more similar to the ideal pseudo-first order model Eq. (1). For this reason, the shape of the binding signal itself is not sufficient to rule out the influence of MTL. (This also highlights again the need for analyte concentrations far above K_D.)

It also follows from (6) that $k_{on}^{(app)} < k_{tr}\,(s_{\max} - s(t))^{-1}$, which means that the fractional saturation reached in the experiment and the transport rate constant impose an absolute upper limit on the apparent rate constant that can possibly be observed in SPR biosensing, irrespective of the true chemical rate constant (see Note 6).

As useful as they are, it is important to recognize that the use of compartment models is highly oversimplifying the physical situation. As mentioned above, if we equate the compartment with physical regions, the spatial parameters within these regions are ignored, since the compartments are well-mixed within. As a consequence, compartment models are not applicable, for example, where the microscopic step of the transport creates significant concentration gradients within the sensing volume, which will occur in the more severely transport influenced binding processes. In fact, due to the very nature of a coupled reaction/diffusion processes, the formation of concentration gradients propagating as moving fronts is a hallmark of the binding process. Such moving fronts of saturation would violate the steady-state assumptions going into the approximation of Eq. (6) (even in more refined multi-compartment models).

That moving fronts of saturation can be present in SPR surface binding has been experimentally verified in three different ways. The First exploits that across the sensing volume the sensitivity of the SPR biosensor is not uniform: laterally it is determined by the shape of the spot being optically interrogated, and perpendicular to the surface it is governed by the evanescent field exponentially decreasing with increasing distance from the surface. Thus, if a moving front of saturation occurs during the association phase, as it moves from the outer regions to the more sensitive inner regions (either laterally or perpendicular to the surface), it will create binding signals with increasing slopes. These have been widely observed (Figure 7) (12, 13), and are difficult to explain with chemical kinetics, even with cooperative binding models. Second, in the experiment we can stop this front of saturation by shutting off the analyte supply and switching to the dissociation phase. If this is done at a point in time when the front is located at a steep gradient of sensitivity, the slow effective diffusion within the matrix of binding sites will transport some analyte from the saturated front into the array of empty sites located ahead in the more sensitive regions, thereby creating an increasing signal component during the dissociation phase – i.e., without net introduction of new analyte to the sensor surface! Simulations of this effect showed that this signal increase can even match or be larger than the loss of signal from the effective dissociation rate (which is slowed due to retention from rebinding) (12). This causes a signature of highly MTL dissociation with slowly decreasing signals following high saturation, but *increasing* signals following partial saturation. Typical experimental profiles

[6]Therefore, as indicated above, the estimates for $k_{on}^{(app)}$, if derived from an empirical application of a pseudo-first-order model, cannot be taken as a measure for estimating the possible extent of MTL, since the latter would require knowledge of the true k_{on}, which may be much higher especially in the presence of MTL.

can be found in the literature (12), and an example studied in our laboratory is shown in Figure 7. Third, the formation of moving fronts of saturation during the electrostatic preconcentration of BSA during the immobilization process has been directly observed with two-color SPR (48), which allows to probe the binding progress in different zones perpendicular to the surface by virtue of the different penetration depths of the evanescent fields of the different wavelengths.

It is important to realize that for severely mass transport limited binding processes with moving fronts the density distribution of surface sites relative to the sensitivity profile of the detection will have a paramount influence on the observed binding profiles. For example, if a majority of sites are at locations of low sensitivity and easily accessible (such as at the top of the immobilization matrix) and a minority of sites are at locations of high sensitivity but require significant additional analyte transport time (such as in the interior of the immobilization matrix), kinetic binding traces may arise under MTL conditions that deviate from the linear initial phase in the association, and instead exhibit more convex shapes in the association phase with some similarity to biphasic exponential binding (15).

3.3. Probing Experimentally for Mass Transport Limitation

As indicated above, the extent of MTL is difficult to predict *a priori* for any given system, since it will depend so much on matrix(or surface)/analyte interactions that are hard to quantify, in addition to the true intrinsic binding rate constants that are generally unknown. Therefore, experimental tools are of critical importance for the detection and moderation of MTL.

An obvious but not very effective way to detect MTL is the variation of the flow rate (see, for example, Figure 8). If a change in the analyte and buffer flow rate in the different experiment phases, respectively, result in differences in the observed surface binding kinetics, MTL is unequivocally demonstrated. Unfortunately, the reverse is not true. As mentioned above, the effective transport rate k_{tr} in the laminar flow depends only on the cube root of the flow rate, which requires very large changes in the flow rate and concomitantly very large increases in the applied volumes (which may be a limiting factor). Further exacerbating this problem is that, as shown in Eq. (6), except for completely mass transport limited cases, we should not expect a change in $k_{on}^{(app)}$ or $k_{off}^{(app)}$ to be proportional to k_{tr}, but to exhibit a weaker influence. Finally, if the microscopic transport step in the matrix is the rate limiting one, the flow rate across the matrix may not show a significant influence on the binding progress.

Nevertheless, it is certainly a good practice to use the highest possible flow rate in order to minimize this transport step. In order to keep the option open to quantitatively analyze the mass transport influenced binding kinetics, it is useful to apply the same flow rate in the association and the dissociation phase of the experiment. The oscillating flow technique can help to strongly reduce the amount of sample required, independently of the flow rate (22).

An alternative approach to probe for the presence of MTL in the laminar flow is the change of the solvent viscosity, for example, by adding glycerol to the buffer (49, 50). Again, an

influence on the observed binding kinetics suggests the presence of MTL. (In principle, there may be some undesired side-effects through differences of protein solvation, as well as the hydration of the immobilization matrix.)

Clearly, the total number of surface sites is an important factor that directly determines the magnitude of MTL, as is reflected in Eq. (6) of the two-compartment model. This led to the approach of comparing the signal from analyte binding to surfaces with different densities of the immobilized binding partner (or, more precisely, different total binding capacities). If the time-course of the analyte binding signal of each surface is normalized relative to the total surface site density, superimposable curves should ideally be obtained in the absence of MTL, whereas in the presence of MTL slower kinetics should be obtained for the higher density surfaces (37). The advantage of this approach is that it will allow equally the detection of MTL arising from the laminar flow, as well as from the microscopic step of diffusion within the matrix. However, a caveat is that this presumes the surface sites exhibiting equal intrinsic binding properties on all surfaces. Unfortunately, this assumption may not always be fulfilled, as we have recently observed in the context of studying the affinity distributions of the ensemble of surface sites (19) (see below).

To minimize the potential influence of MTL it is prudent to aim for low surface site densities, although not to the extent of sacrificing reasonable signal/noise ratio (see above). Similarly, in our experience it can be advantageous to use thin immobilization matrices, which usually accommodate sufficient numbers of molecules to generate adequate signal levels.

In many cases perhaps the best strategy to diagnose the presence of MTL is the use of a soluble competitor in the dissociation phase, which binds to the analyte once dissociated and prevents it from rebinding to the empty surface sites (51). If the binding reaction under study is mass transport limited, the competitor can dramatically increase the dissociation rate, in particular when applied at a point in time when half or more of the surface sites are already (or still) unoccupied. There can be potential concern with very large competitors that may not be able to penetrate the matrix well and not diffuse well into the rebinding zone. A significant advantage of this approach is that it can allow to estimate the intrinsic chemical off-rate constant, provided the concentration of the competitor should be sufficiently high to lead to essentially stoichiometric capture of all analyte molecules as they are released from the surface sites (2). This may be combined with the equilibrium constant from the analysis of the steady-state surface binding isotherm to provide an estimate of the true on-rate constant.

Ideally, we recommend to use all or a combination of several of these techniques to diagnose the presence of MTL in the measured binding kinetics.

3.4. Incorporating Mass Transport Influence into the Model of the Binding Kinetics

Unfortunately, given the complexity of the physico-chemical phenomena at the sensor surface and in the immobilization matrix, it seems highly unrealistic to even establish a complete physical model for the transport process that incorporates all the relevant processes, not to speak of determining all the necessary parameters. This becomes evident

considering only the problem that we would need to know the spatial distribution of the immobilized surface sites. Making assumptions about these parameters is an important and valid tool to explore their possible influence, but it would lead to unreliable and to a high degree arbitrary results when used for the analysis of MTL data.

Some authors have studied the mass transport problem confining their attention to the laminar flow, which is a simpler problem and more tractable, and suggested it would be possible to predict the mass transport rate constant on the basis of the known geometry of the flow and the analyte diffusion constant (52). However, as we have demonstrated elsewhere using a commonly available antibody/antigen system, the experimental transport rate constants can be far off the predicted values dependent on the immobilization matrix used (13).

Due to these difficulties, it seems reasonable only to attempt the application of the simplest phenomenological compartment model for transport, and to restrict the usage of this model to just the onset of mass transport limitation where the spatial concentration gradients are small, and the approximation of the spatial geometry by a simple division into two regions is tolerable to serve as a first approximation. Alternatively, it may be applied in the limit of the approach to steady-state in the association phase, where existing gradients have decayed (49). Since there are several physical processes affecting the transport with unknown relative importance (dependent on the interacting system and the matrix properties), we can use an effective overall transport rate constant $k_{tr}^{(app)}$, which will arise as a harmonic mean of effective transport rate constants of many different sequential transport steps (13). Because we cannot predict the value of $k_{tr}^{(app)}$ without making assumptions of uncertain validity, it needs to be incorporated as an adjustable parameter into the data analysis.

At low influence of MTL, i.e. in the reaction limited regime, the value of $k_{tr}^{(app)}$ will not be well determined by the data, except that we can establish a lower limit of $k_{tr}^{(app)}$. However, the rate constants of the chemical reaction of interest is well determined. *Vice versa*, in the limit of high influence of MTL, the value of $k_{tr}^{(app)}$ may be well-determined by the data, but we can only estimate a lower limit of the chemical on-rate constant.

In practice, Eq. 5 can be fit directly globally to the set of association/dissociation phases from a single site model. The two-compartment transport step outlined in Eq. 5 may also be combined with other, more complex models for the chemical binding step. For more strongly MTL surface binding reactions, we observed in a computer model of transport within the immobilization matrix that the spatial gradients in the dissociation phase are smaller than in the association phase. This suggests that the application of Eq. 6 to the set of dissociation phases, which leads to the compact form

$$\frac{ds(t)}{dt} = \frac{-k_{off}\, s(t)}{1 + \frac{k_{on}}{k_{tr}}(s_{\max} - s(t))} \quad (7)$$

may be a more robust approach (see e.g., (49, 50)) to estimate the chemical off-rate constant. This could be combined with the equilibrium constant derived from the steady-state isotherm to provide estimates for the chemical on-rate constant.

It should be noted that for the analysis of MTL binding traces, the data reporting on the kinetics under the condition of high site occupancy are the most informative. Therefore, Eqs. (5) or (7) are applied best to data sets that include concentrations far above K_D.

4. Heterogeneity of the Surface Sites

4.1. Physical Origin

The need to immobilize one of the binding partners of the interaction to be studied raises another problem fundamental to biosensing. Obviously, we want to assume (and if possible verify) that the immobilization itself does not significantly influence the molecular binding parameters. This may not always be trivial, considering general experience with labeling of proteins, the SPR surface being nothing less than a macroscopic-sized label. In addition, however, a less obvious but equally important assumption is that all immobilized sites are uniformly active (and a fraction may be completely inactive, respectively, which would not contribute to the binding signal). Considering the physical microheterogeneity of any SPR surface on a molecular scale (even without polymer matrices), the different local chemical properties of the surface, the possible geometric configurations of the immobilized sites relative to the surface and relative to the molecules comprising the immobilization matrix, possible heterogeneity in the protein conformations, in addition to the common chemical heterogeneity in the covalent attachment, it seems actually a very daunting task to achieve uniformity in the binding properties of the immobilized macromolecules. This is true even for preparations that in solution exhibit properties consistent with a single class of sites.

Although there are strategies to avoid some sources of heterogeneity, such as the surface attachment by site-directed chemistries or capture techniques, these cannot address other problems arising from the physical and chemical microheterogeneity of the surface itself as well as the immobilization matrix (if used) (Figure 9).

As a consequence, it seems a much more sensible assumption that the immobilized surface sites could present a distribution exhibiting a continuum of binding energies. This naturally incorporates the possibility for partially active sites, non-specific sites, as well as multiple independent sites on the immobilized molecules.

4.2. Description of Analyte Binding to an Ensemble of Surface Sites with a Distribution of Rate and Affinity Constants

We can express the idea that the observed binding signal is the sum of signals from sites that could have different dissociation equilibrium constants and different off-rate constants as an integral equation

$$s_{tot}(c,t)=\int_{K_{D,\min}}^{K_{D,\max}}\int_{k_{off,\min}}^{k_{off,\max}} s_1(k_{off},K_D,c,t)P(k_{off},K_D)dk_{off}dK_D \quad (8)$$

where $s_1(k^*_{off},K^*_D,c,t)$ is the binding signal we would observe for a site with equilibrium constant K^*_D and off-rate constant k^*_{of} at a unit binding capacity of $s_{\max}(k^*_{off},K^*_D)=1$, following Eqs. (2) – (4), and where $P(k_{off},K_D)$ is the two-dimensional distribution of affinity and rate constants (53). This model, with the features described below, has been implemented in the software EVILFIT, and is available from the authors on request.

It is well-known that the decomposition of experimental data into a distribution of exponentials is an ill-posed problem (54), and the analysis of SPR surface binding data is no exception. This is because within a given level of noise, single exponentials for example are poorly distinguishable from a combination of two exponentials of lower and higher exponents. In practice, this leads to the amplification of noise in the data to the extent that it can govern the overall distribution. As a consequence, if Eq. (8) were fitted directly to experimental data, the best-fit distribution would likely be a series of poorly reproducible spikes, which would present much more detailed features than information really contained in the original data. A very powerful modern approach to address this problem, termed ‘regularization’, follows the principle of Occam’s razor that suggests that the simplest possible interpretation of the data is most likely the right one. It is implemented by defining a mathematical measure of information content of the final distribution, and aims at minimizing this information content as much as possible without decreasing the quality of fit to the raw data (as judged by statistical analysis of the residuals). It results in the simplest, or broadest distribution consistent with the experimental data.

This provides a very convenient way to assess the information content of the experimental SPR data (19, 53): For example, when applied to data consisting of a single association/dissociation trace, data at concentrations $\ll K_D$, data at very low signal/noise ratio, or otherwise poorly designed experiments, the distribution of affinity and off-rate constants shows broad peaks reflecting the limited conclusions that can be drawn from the experiment. In contrast, when applied to data from a better designed experiment, the peaks in the distribution become sharp and allow more detailed insight in the surface binding process. This is illustrated in Figure 10, which shows the affinity and rate constant distribution for the interaction of the same analyte to an identical surface, once with very short association and dissociation times (left) and once with a larger analyte concentration range and longer observation times in both the association and dissociation phase.

When applied to suitable data, the level of detail that can be observed on the functional distribution of surface binding sites is high, and, as shown in (19), the distributions are quite reproducible. It is possible to clearly distinguish the high-affinity sites of interest from subpopulations of sites with impaired affinity, which possibly reflect protein immobilized in altered conformations and/or in poorly accessibly locations on the surface in the immobilization matrix, and from low-affinity sites, which may be intrinsic to the surface (non-specific binding of analyte to the surface) or reflect residual weak interactions with

denatured proteins. By discriminating the different populations, it is possible to focus on the interaction of interest, and to obtain binding parameter estimates that are not skewed by subpopulations of partially inactive or non-specific surface sites. If there is a doubt about which of the peaks reflects the 'native' interaction, we recommend to conduct solution competition assays to measure the affinity constant in solution (21, 33) (see also Chapter de Mol).

Since the standard regularization causes peaks to be as broad as consistent within the signal/noise level of the experimental data, it is not immediately clear whether a single species model would be consistent with the data. To this end, a Bayesian approach can be taken to reshape the regularization profile towards favoring distributions consistent with prior knowledge (or prior hypothesis) (19). To examine to what degree given data are consistent with a single site model, suitable prior knowledge may be bootstrapped from experimental data by performing a preliminary analysis with conventional regularization, followed by integration over the distribution region in question (which possibly may represent a single species), and assigning the prior knowledge for the following Bayesian analysis to be a sharp peak with the signal-average binding constants from the relevant region. The result will be the affinity and rate constant distribution that resembles as close as possible a single-site model, given the experimental data. In contrast to the direct application of (1) – (4) that would strictly constrain the fit to a single-site model and cause (in virtually all cases when applied to meaningful data) a statistically unacceptable fit, this Bayesian approach will not diminish the quality of fit from the best possible fit with the full distribution model and instead add features to the putative single species model that are essential to explain the actually observed data. These additional features may be populations of low-affinity sites, or poorly reversible sites.

The Bayesian approach was applied with the EVILFIT software (freely available from the authors on request), for example, to the data in Figure 2 in order to test for the homogeneity of the surface sites. The result clearly shows that the hypothesis of a single homogeneous binding site for the main peak cannot be accommodated in the fit of the experimental data. Instead, the distribution highlights that there must be microheterogeneity of the surface sites. This validates the physical picture sketched in Figure 9 where microheterogeneity in the local physical and chemical environment of the immobilized molecules, as well as chemical and/or conformational heterogeneity from surface attachment creates polydispersity of the binding energies, and therefore subpopulations of different affinity and rate constants for analyte binding. For the data shown in Figure 10, this – in addition to trace populations of low affinity sites and poorly reversible sites – explains the deviation of the binding progress curves from the single exponential ideally expected.

Independent of the interpretation of the resulting distribution, another important observation from the distribution model is the high quality of fit. This is consistent with the generally excellent stability and reproducibility of SPR biosensor data. From our experience applying this model to many systems, it is possible routinely (but not always) to achieve fits with residuals satisfactorily within the noise of the data acquisition. This is very significant in that it on one hand suggests the validity of the model and its underlying assumptions (provided the data set is collected with meaningful design), and on the other hand sets the bar for a

satisfactory data interpretation back to the same criteria used in most other biophysical disciplines, where systematic deviations between data and fit are simply taken to reject the model. The same rational conclusion can and should be drawn when analyzing SPR data. We do believe that when the best-fit is significantly worse, one should conclude that the model does not reflect the binding process actually taking place. This may require the combination with MTL corrections, as described below, or reflect the fact that the assumption of independent parallel 1:1 binding events of uniform analyte molecules does not apply.

5. Relationship between mass transport and surface heterogeneity

We have discussed above the two most common sources of deviation from ideal single-exponential pseudo-first order surface binding. In practice, MTL and surface heterogeneity are related problems, since both are governed by the density, spatial distribution, and detailed local properties of the immobilized surface sites.

Any of the surface sites, whether reflecting the ‘native’ binding properties or artificial low-affinity or ‘non-specific’ sites, will contribute to the depletion and retention, respectively, of analyte in the vicinity of the sensor surface, and thereby diminish the effective transport rate and increase MTL. This causes the surface binding to the different surface sites be a coupled process: Analyte molecules dissociating from one class of sites may re-bind to another site with different affinity and kinetic constants.

Fortunately, the effect of MTL and surface heterogeneity on the shape of the observed surface binding traces is opposite: MTL often causes less convex binding kinetics (more linear) in the association phase, whereas surface heterogeneity typically causes more convex traces in the association phase. The effect on the shape of the dissociation phase is similar in that both appear multi-phasic, but with different concentration dependence. For this reason, MTL and surface heterogeneity do not correlate much and can be distinguished in the analysis of experimental data.

Mathematically, the combined effects of surface heterogeneity and MTL can be expressed with the system of rate equations

$$\begin{aligned} \frac{dc_{surf}}{dt} &= k_{tr}(c - c_{surf}) - \frac{ds}{dt} \\ \frac{ds_i}{dt} &= k_{on,i} c_{surf}(P_i(k_{off,i}, K_{D,i}) - s_i) - k_{off} s_i \end{aligned} \quad (9)$$

where the sum of all binding signals to each population i is the total measured signal, $s(c,t) = \Sigma_i s_i(c,t)$, and the population $P_i(k_{off,i},K_{D,i})$ of each site gives a discretized representation of the affinity and kinetic rate constant distribution (13). Such a model was applied, for example, for the global analysis of the data shown in Figure 8. This model assumes a single transport rate constant for binding to all sites. This may strictly not always be fulfilled, for example, to account for binding inside or outside the immobilization matrix. Unfortunately, accounting for such an effect seems to exceed current computational capabilities in the data analysis and likely the information content of experimental surface binding data.

Since MTL depends strongly on the total number of surface sites, a popular approach to diagnose the presence of and to quantitatively account for MTL has been the comparison of analyte binding kinetics to surfaces at different total immobilization density (or rather different binding capacity). However, this is based on the silent assumption that the binding properties of the surface sites do not change for the different surfaces. With the availability of the surface site distribution analysis it is possible to test this assumption. Figure 11 shows the functional surface site distribution for two different antibody-antigen systems. The system shown in Panels A and B exhibits very similar affinity and kinetic distributions when immobilized at different levels. In contrast, the other system shown in Panels C and D exhibits a significant shift towards a higher affinity population at the higher immobilization density. This highlights that the immobilization process, dependent on the macromolecular system under study, may indeed create different subpopulations of sites at different stages of the immobilization process.

This could be related to the intrinsic heterogeneity of the surface, in particular when using an immobilization matrix, and the fact that the immobilization process itself is a kinetic process requiring mass transport, likely being mass transport limited itself. One could easily imagine that the resulting spatial distribution of the immobilized surface sites will not be uniform, and therefore create different amounts of subpopulation in different microenvironments with different binding properties.

Another possible mechanism for a dependence of the affinity distribution on the total immobilization density could involve the oligomerization of the immobilized macromolecules. Contributing factors for oligomerization are the high local concentrations (routinely in the 1 – 10 mg/ml range or higher inside the matrix) and the increased propensity of protein oligomerization in the presence of a surface (55) as well as volume-excluding polymers (56). In particular for proteins undergoing self-association in solution, this may be a likely scenario.

In practice, concerns of MTL and surface heterogeneity must both be kept in mind and may have to be balanced when deciding on the strategy of surface immobilization. For example, the use of proteins for site-specific capture of the binding partner of interest, such as antibodies or streptavidin, may improve the chemical homogeneity of the surface sites, but at the same time make the surface more sticky and dense, and thereby hamper diffusion and create stronger MTL. Conversely, the use of no or very short polymer supports for immobilization matrices can eliminate longer diffusion distances and improve MTL, but may not screen as well non-specific binding sites (e.g., driven by hydrophobic interactions) directly at the surface, and thereby increase the heterogeneity of the measured affinity distribution.

This is not to suggest that both could not be minimized simultaneously, but just to highlight how they are interrelated fundamentally due to the need for immobilization to the surface of one of the binding partners to be characterized. If the initial rate or the steady-state signal of SPR surface binding is only taken as an empirically calibrated signal reporting on the concentration of free analyte, and this surface binding assay is used to probe the solution

equilibrium constant in the presence of soluble competitors to the surface sites, both problems of MTL and surface heterogeneity become irrelevant.

6. Conclusions

The present chapter was meant as an introduction to the strategies for the kinetic analysis of SPR surface binding data, and two major problems arising in the surface binding format. The brief history of SPR biosensing in the biomedical sciences cautions us that the correct interpretation of kinetic surface binding traces as reflecting molecular parameters, rather than merely being a reflection of the often complex properties of the particular surface generated, is not trivial at all. The most important requirements for a reliable characterization of molecular parameters are: (1) the design of experiments that will provide meaningful information on the desired parameters and allows us to discriminate between chemical binding of interest and artifact, (2) the application of stringent tests of the consistency of the model and the data, (3) the critical awareness of the assumptions made in the analysis, and (4) the design and application of experimental controls to test these assumptions.

This is especially important when the binding traces do not follow the simplest possible binding process, that of a single site with pseudo-first order binding kinetics. Two simple reasons for deviations that are fundamentally related to SPR biosensing (rather than primarily the molecules of interest) are MTL and surface heterogeneity. We have introduced tools that help to address both problems and to obtain, despite their presence, estimates for the affinity and kinetic parameters of the molecular interaction to be studied. Using the model that accounts for surface heterogeneity, fits can often be achieved that describe the experimental within the noise of data acquisition. This should be the goal of the kinetic analysis, and failure to meet this criterion should lead us to reject the hypothesis underlying the data analysis.

We have not discussed advanced questions of how to further improve the model if the consideration of the two most common surface-related problems cannot explain the data. Glaser & Hausdorf (32) have studied a model system exhibiting multi-phasic binding and noted the difficulty that many different more complex binding models fitted the data equally well. This is exacerbated by the fact that the problems of surface heterogeneity and MTL will likely be superimposed to more complex chemical kinetics. The recently discovered apparently ubiquitous presence of surface site heterogeneity, in particular, would make the reliable identification of a complex reaction scheme much more difficult. Even if the reaction scheme is known from other techniques, the determination of its associated molecular binding parameters could be highly problematic. In such situations, it seems more appealing to constrain the quantitative data analysis to the interpretation of the steady-state responses as a function of analyte concentration towards estimating equilibrium binding constants. Alternatively, the solution competition approach may provide solution affinity constants (see Chapter de Mol). In some cases of more complicated binding reactions between two or more molecules, it is also possible to use the SPR surface binding assay to at least answer qualitative questions about the binding scheme, presence of cooperativity, etc. (6). This is a very powerful aspect of the application of SPR surface binding which seems

sometimes under-appreciated, but can often provide reliable and critical information about the mechanism of protein interactions.

Acknowledgments

This research was supported by the Intramural Research Program of the National Institute of Bioengineering and Physical Science, National Institutes of Health.

References

1. Fägerstam LG, Frostell Å, Karlsson R, et al. Detection of antigen-antibody interactions by surface plasmon resonance. Application to epitope mapping. J Mol Recogn. 1990; 3:208–214.
2. Schuck P. Use of surface plasmon resonance to probe the equilibrium and dynamic aspects of interactions between biological macromolecules. Ann Rev Biophys Biomol Struct. 1997; 26:541–566. [PubMed: 9241429]
3. Cooper MA. Optical biosensors in drug discovery. Nat Rev Drug Discov. 2002; 1:515–28. [PubMed: 12120258]
4. Pattnaik P. Surface plasmon resonance: applications in understanding receptor-ligand interaction. Appl Biochem Biotechnol. 2005; 126:79–92. [PubMed: 16118464]
5. Schasfoort, RBM.; Tudos, AJ. Handbook of Surface Plasmon Resonance. Cambridge: RSC Publishing; 2008.
6. Sundberg, EJ.; Andersen, PS.; Gorshkova; Schuck, P. Surface plasmon resonance biosensing in the study of ternary systems of interacting proteins. In: Schuck, P., editor. Protein Interactions: Biophysical Approaches for the Study of Complex Reversible Systems. Vol. 5. New York: Springer; 2007. p. 97-141.
7. Krone JR, Nelson RW, Dogruel D, Williams P, Granzow R. BIA/MS: interfacing biomolecular interaction analysis with mass spectrometry. Anal Biochem. 1997; 244:124–32. [PubMed: 9025918]
8. Sonksen CP, Nordhoff E, Jansson O, Malmqvist M, Roepstorff P. Combining MALDI mass spectrometry and biomolecular interaction analysis using a biomolecular interaction analysis instrument. Anal Chem. 1998; 70:2731–6. [PubMed: 9666738]
9. Natsume T, Nakayama H, Jansson O, Isobe T, Takio K, Mikoshiba K. Combination of biomolecular interaction analysis and mass spectrometric amino acid sequencing. Anal Chem. 2000; 72:4193–8. [PubMed: 10994983]
10. Gilligan JJ, Schuck P, Yergey AL. Mass spectrometry after capture and small-volume elution of analyte from a surface plasmon resonance biosensor. Anal Chem. 2002; 74:2041–7. [PubMed: 12033305]
11. Mehlmann M, Garvin AM, Steinwand M, Gauglitz G. Reflectometric interference spectroscopy combined with MALDI-TOF mass spectrometry to determine quantitative and qualitative binding of mixtures of vancomycin derivatives. Anal Bioanal Chem. 2005; 382:1942–8. [PubMed: 15983762]
12. Schuck P. Kinetics of ligand binding to receptor immobilized in a polymer matrix, as detected with an evanescent wave biosensor. I A computer simulation of the influence of mass transport. Biophys J. 1996; 70:1230–1249. [PubMed: 8785280]
13. Svitel J, Boukari H, Van Ryk D, Willson RC, Schuck P. Probing the functional heterogeneity of surface binding sites by analysis of experimental binding traces and the effect of mass transport limitation. Biophys J. 2007; 92:1742–1758. [PubMed: 17158569]
14. Karlsson R. Real-time competitive kinetic analysis of interactions between low-molecular-weight ligands in solution and surface-immobilized receptors. Anal Biochem. 1994; 221:142–151. [PubMed: 7985785]
15. Schuck P. Reliable determination of binding affinity and kinetics using surface plasmon resonance biosensors. Curr Opin Biotechnology. 1997; 8:498–502.
16. Langmuir I. The adsorption of gases on plane surfaces of glass, mica and platinum. J Am Chem Soc. 1918; 40:1361–1403.

17. Myszka DG. Improving biosensor analysis. J Mol Recognit. 1999; 12:279–284. [PubMed: 10556875]
18. Ober RJ, Ward ES. The influence of signal noise on the accuracy of kinetic constants measured by surface plasmon resonance experiments. Anal Biochem. 1999; 273:49–59. [PubMed: 10452798]
19. Gorshkova II, Svitel J, Razjouyan F, Schuck P. Bayesian analysis of heterogeneity in the distribution of binding properties of immobilized surface sites. Langmuir. 2008; 24:11577–11586. [PubMed: 18816013]
20. Schuck P, Minton AP. Minimal requirements for internal consistency of the analysis of surface plasmon resonance biosensor data. Trends in Biochem Sci. 1996; 252:458–460. [PubMed: 9009825]
21. Schuck P, Millar DB, Kortt AA. Determination of binding constants by equilibrium titration with circulating sample in a surface plasmon resonance biosensor. Anal Biochem. 1998; 265:79–91. [PubMed: 9866711]
22. Abrantes M, Magone MT, Boyd LF, Schuck P. Adaptation of the Biacore X surface plasmon resonance biosensor for use with small sample volumes and long contact times. Anal Chem. 2001; 73:2828–2835. [PubMed: 11467523]
23. Karlsson R, Katsamba PS, Nordin H, Pol E, Myszka DG. Analyzing a kinetic titration series using affinity biosensors. Anal Biochem. 2006; 349:136–47. [PubMed: 16337141]
24. Ober RJ, Ward ES. The choice of reference cell in the analysis of kinetic data using BIACORE. Anal Biochem. 1999; 271:70–80. [PubMed: 10361006]
25. Karp NA, Edwards PR, Leatherbarrow RJ. Analysis of calibration methodologies for solvent effects in drug discovery studies using evanescent wave biosensors. Biosens Bioelectron. 2005; 21:128–34. [PubMed: 15967360]
26. Ladbury JE, Lemmon MA, Zhou M, Green J, Botfield MC, Schlesinger J. Measurement of the binding of tyrosyl phosphopepdites to SH2 domains: A reappraisal. Proc Natl Acad Sci USA. 1995; 92:3199–3203. [PubMed: 7536927]
27. Muller KM, Arndt KM, Pluckthun A. Model and simulation of multivalent binding to fixed ligands. Anal Biochem. 1998; 261:149–58. [PubMed: 9716417]
28. Davis SJ, Ikemizu S, Wild MK, van der Merwe PA. CD2 and the nature of protein interactions mediating cell-cell recognition. Immunological Reviews. 1998; 163:217–236. [PubMed: 9700513]
29. Andersen PS, Lavoie PM, Sekaly RP, et al. Role of the T cell receptor alpha chain in stabilizing TCR-superantigen-MHC class II complexes. Immunity. 1999; 10:473–483. [PubMed: 10229190]
30. Schuck, P.; Boyd, LF.; Andersen, PS. Measuring protein interactions by optical biosensors. In: Coligan, JE.; Dunn, BM.; Ploegh, HL.; Speicher, DW.; Wingfield, PT., editors. Current Protocols in Protein Science. Vol. 2. New York: John Wiley & Sons; 1999. p. 20.2.1-20.2.21.
31. Brown PH, Balbo A, Schuck P. A bayesian approach for quantifying trace amounts of antibody aggregates by sedimentation velocity analytical ultracentrifugation. Aaps J. 2008; 10:481–93. [PubMed: 18814037]
32. Glaser RW, Hausdorf G. Binding kinetics of an antibody against HIV p24 core protein measured with real-time biomolecular interaction analysis suggest a slow conformational change in antigen p24. J Immunol Methods. 1996; 189:1–14. [PubMed: 8576571]
33. Nieba L, Krebber A, Pluckthun A. Competition BIAcore for measuring true affinities: large differences from values determined from binding kinetics. Anal Biochem. 1996; 234:155–65. [PubMed: 8714593]
34. Krishnamoorthy G, Carlen ET, Kohlheyer D, Schasfoort RB, van den Berg A. Integrated Electrokinetic Sample Focusing and Surface Plasmon Resonance Imaging System for Measuring Biomolecular Interactions. Anal Chem. 2009
35. van der Merwe PA, Barclay AN, Mason DW, et al. Human cell-adhesion molecule CD2 binds CD58 (LFA-3) with a very low affinity and an extremely fast dissociation rate but does not bind CD48 or CD59. Biochemistry. 1994; 33:10149–10160. [PubMed: 7520278]
36. Hall DR, Cann JR, Winzor DJ. Demonstration of an upper limit to the range of association rate constants amenable to study by biosensor technology based on surface plasmon resonance. Anal Biochem. 1996; 235:175–184. [PubMed: 8833325]

37. Glaser RW. Antigen-antibody binding and mass transport by convection and diffusion to a surface: A two-dimensional computer model of binding and dissociation kinetics. Anal Biochem. 1993; 213:152–161. [PubMed: 8238868]
38. Lok BK, Cheng Y-L, Robertson CR. Protein adsorption on crosslinked polydimethylsiloxane using total internal reflection fluorescence. J Coll Interface Sci. 1983; 91:104–116.
39. Gedig, E. Surface chemistry in SPR technology. In: Schasfoort, RBM.; Tudos, AJ., editors. Handbook of Surface Plasmon Resonance. Cambridge: The Royal Society of Chemistry; 2008. p. 173-220.
40. Stenberg E, Persson B, Roos H, Urbaniczky C. Quantitative determination of surface concentration of protein with surface plasmon resonance using radiolabeled proteins. J Coll Interface Sci. 1991; 143:513–526.
41. Yeung D, Gill A, Maule CH, Davies RJ. Detection and quantification of biomolecular interactions with optical biosensors. Trends in Analytical Chemistry. 1995; 14:49–56.
42. Crank, J. The mathematics of diffusion. Oxford: Clarendon Press; 1975.
43. Yarmush ML, Patankar DB, Yarmush DM. An analysis of transport resistances in the operation of BIAcore; Implications for kinetic studies of biospecific interactions. Mol Immunol. 1996; 33:1203–1214. [PubMed: 9070669]
44. Pero JK, Haas EM, Thompson NL. Size dependence of protein diffusion very close to membrane surfaces: measurement by total internal reflection with fluorescence correlation spectroscopy. J Phys Chem B Condens Matter Mater Surf Interfaces Biophys. 2006; 110:10910–8. [PubMed: 16771344]
45. de Gennes PG. Conformation of polymers attached to an interface. Macromolecules. 1980; 13:1069–1075.
46. Xu F, Persson B, Lofas S, Knoll W. Surface plasmon optical studies of carboxymethyl dextran brushes versus networks. Langmuir. 2006; 22:3352–7. [PubMed: 16548600]
47. Balgi G, Leckband DE, Nitsche JM. Transport effects on the kinetics of protein-surface binding. Biophys J. 1995; 68:2251–2260. [PubMed: 7647232]
48. Zacher T, Wischerhoff E. Real-time two-wavelength surface plasmon resonance as a tool for the vertical resolution of binding processes in biosensing hydrogels. Langmuir. 2002; 18:1748–1759.
49. Schuck P, Minton AP. Analysis of mass transport limited binding kinetics in evanescent wave biosensors. Anal Biochem. 1996; 240:262–272. [PubMed: 8811920]
50. de Mol NJ, Plomp E, Fischer MJ, Ruijtenbeek R. Kinetic analysis of the mass transport limited interaction between the tyrosine kinase lck SH2 domain and a phosphorylated peptide studied by a new cuvette-based surface plasmon resonance instrument. Anal Biochem. 2000; 279:61–70. [PubMed: 10683231]
51. DeLisi C. The biophysics of ligand-receptor interactions. Q Rev Biophys. 1980; 13:201–230. [PubMed: 7015404]
52. Myszka DG, He X, Dembo M, Morton TA, Goldstein B. Extending the range of rate constants available from BIACORE: interpreting mass transport-influenced binding data. Biophys J. 1998; 75:583–94. [PubMed: 9675161]
53. Svitel J, Balbo A, Mariuzza RA, Gonzales NR, Schuck P. Combined affinity and rate constant distributions of analyte or ligand populations from experimental surface binding and kinetics and equilibria. Biophys J. 2003; 84:4062–4077. [PubMed: 12770910]
54. Provencher SW. Inverse problems in polymer characterization: Direct analysis of polydispersity with photon correlation spectroscopy. Makromol Chem. 1979; 180:201–209.
55. Minton AP. Effects of excluded surface area and adsorbate clustering on surface adsorption of proteins. II Kinetic models. Biophys J. 2001; 80:1641–8. [PubMed: 11259279]
56. Zimmerman SB, Minton AP. Macromolecular crowding: Biochemical, biophysical, and physiological consequences. Annu Rev Biophys Biomol Struct. 1993; 22:27–65. [PubMed: 7688609]
57. Karlsson R, Michaelsson A, Mattson L. Kinetic analysis of monoclonal antibody-antigen interactions with a new biosensor based analytical system. J Immunol Methods. 1991; 145:229–240. [PubMed: 1765656]

58. Roden LD, Myszka DG. Global analysis of a macromolecular interaction measured on BIAcore. Biochem Biophys Res Commun. 1996; 225:1073–1077. [PubMed: 8780736]

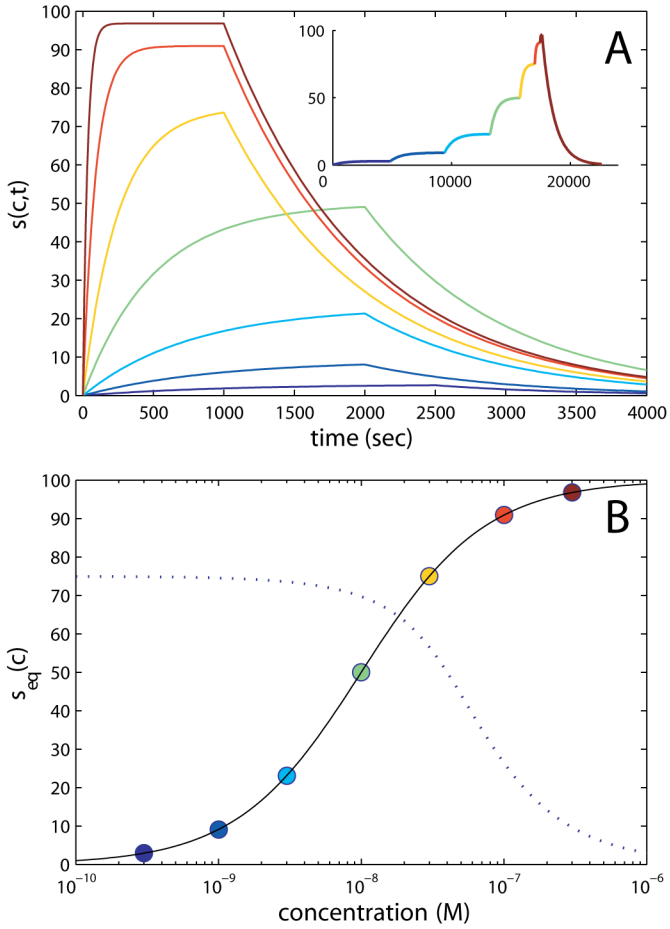

Figure 1.

Surface plasmon resonance biosensor signal ideally expected for a simple 1:1 interaction with pseudo-first order kinetics, in different experimental configurations: (A) This is a superposition of sensorgrams in the kinetic configuration most commonly used, where the association/dissociation cycles at different concentrations are separated by regeneration steps. The data shown are generated for the binding of molecules with a K_D of 10 nM (k_{on} = 1.0×10^5 $M^{-1}s^{-1}$ and $k_{off} = 1.0 \times 10^{-3}$ s^{-1}) probed with a range of analyte concentrations (0.3 nM navy, 1 nM blue, 3 nM cyan, 10 nM green, 30 nM orange, 100 nM red, and 300 nM dark red). In order to approach more closely the equilibrium signal at the lower concentrations, the contact time for the lowest concentration cycles is increased. The inset shows an alternative kinetic titration configuration in which the signal from bound material is continuously accumulated by applying a step-wise increased analyte concentrations, followed by only a single dissociation phase. This has the advantage of not requiring a regeneration step, but at the cost of lower information content (see text). The colors of the curve depict the equivalent concentrations as the main plot. (B). The equilibrium binding constant can be determined independent of the kinetics, by evaluating the extrapolated steady-state signals as a function of concentration (filled circles, using the same color scheme as in A), which follows a Langmuir isotherm (solid line). The dotted line presents an isotherm from a solution competition assay, in which the sample solution contains analyte at

a constant concentration (at $2\times K_D$) mixed with a varying concentration of soluble ligand competing for the surface sites (see Chapter de Mol). This strategy utilizes the SPR surface sites to report on the remaining free analyte in solution for the different mixtures applied in the flow, and yields binding constants for the interaction in solution. It can be combined with an empirically constructed calibration curve of SPR binding signal *vs* free analyte concentration. In this latter configuration, no assumptions on the property of the surface binding sites are necessary.

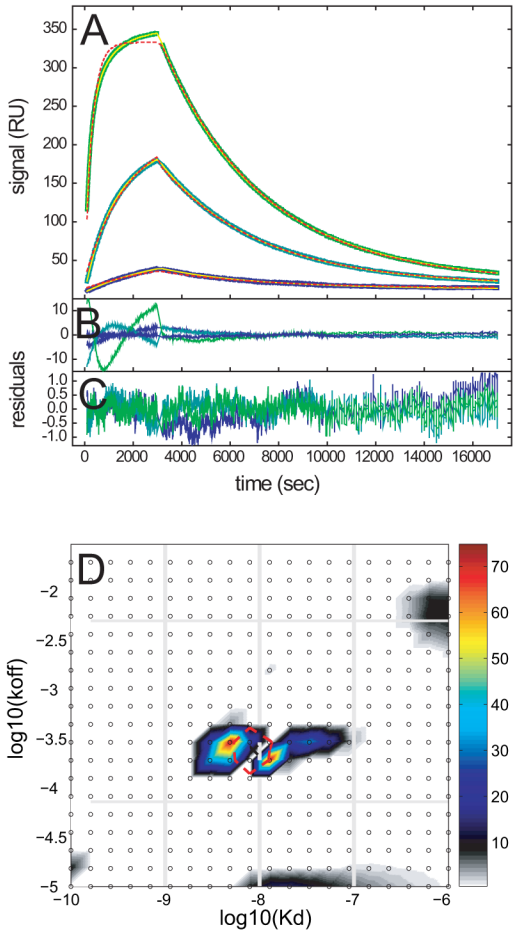

Figure 2.

Typical example for the inability of single-site model in describing the surface binding data, due to the presence of heterogeneity of binding sites on the surface. This is binding of an antigen to its monoclonal antibody immobilized on a short-chain carboxy-methyl dextran surface. For details, see (19). (A) Experimental binding traces at analyte concentrations of 1 (navy), 10 (blue) and 100 nM (green), best-fit traces using the surface site distribution model (solid yellow line), and best-fit curves from a single-site model (dashed red line). (B) Residuals of the fit from the single-site model, with an rmsd of 3.42 RU. (C) Residuals of the fit from the Bayesian distribution model shown in D, with an rmsd of 0.31 RU. (D) Affinity and rate constant distribution calculated using the Bayesian analysis to obtain the distribution closest to a single class of sites with average parameters (encircled by the red dashed line). The distribution is depicted as a color temperature contour plot, with the colors indicating the signal values shown in the color bar at the right. Also shown in the distribution plot are the concentrations applied in the experiment (vertical gray lines), and the rate constants that could be well characterized within the experimental dissociation time (horizontal gray lines).

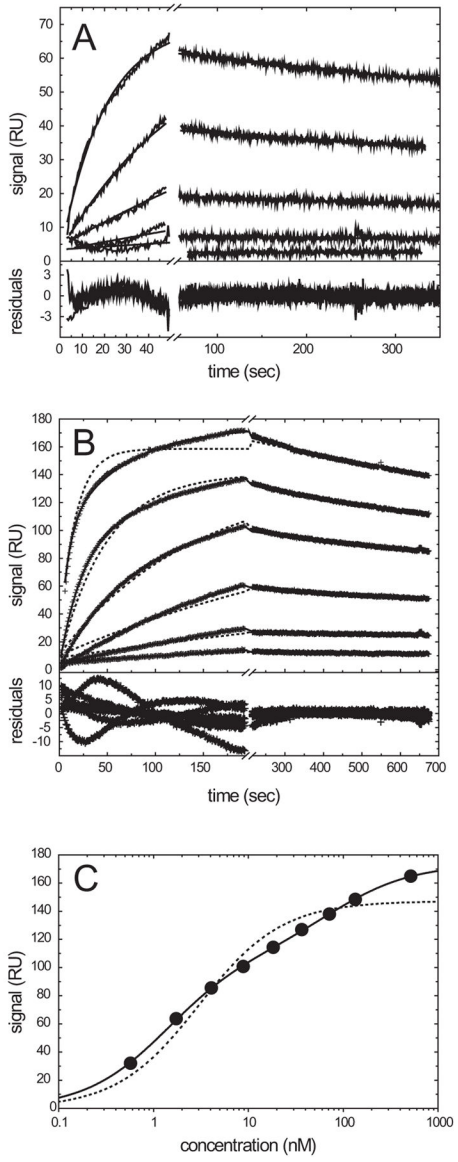

Figure 3.

Demonstration how the arbitrary truncation of the data acquisition can lead to qualitative misinterpretation of the binding kinetics. Shown are kinetic binding signals of myoglobin binding to immobilized antibody. (A) Roden & Myszka (58) used this model system in their study aimed at demonstrating that SPR surface binding data follow simple bimolecular binding to a single class of sites, without complications arising from factors such as the immobilization matrix and mass transport. They developed an experimental design that uses analyte at four concentrations and is restricted to acquire association data for only 42 sec. The data shown in (A) are very similar to those presented by Roden & Myszka, and lead to binding rate constants of $k_{on} = 1.9 \times 10^5\ M^{-1}s^{-1}$, $k_{off} = 3.98 \times 10^{-4}\ s^{-1}$, very close to those reported by Roden & Myszka of $k_{on} = 1.94 \times 10^5\ M^{-1}s^{-1}$, $k_{off} = 4.70 \times 10^{-4}\ s^{-1}$. Indeed, a good fit is achieved with this model. However, the low degree of curvature in the kinetic traces severely limits the information content. (B) Binding data using a more informative

experimental design that features a considerably longer association phase and an extended range of analyte concentrations. Here, the global kinetic analysis using the pseudo-first order model (dotted line) does not lead to an acceptable fit, as it is unable to describe the slower binding phase that becomes apparent at contact times > 50 sec. Since the data are from the same surface, it clearly shows that the restricted data collection in (A) led to the gross misinterpretation of the data. (C) An equilibrium binding isotherm using the equilibrium titration method described in (21) and obtained from the same surface reveals a biphasic isotherm, which cannot be explained on the basis of a single class of sites (dotted line), but can be modeled well with two classes of sites (solid line). Best-fit parameters are $K_{D,1}$ = 1.4 nM (63%) and $K_{D,2}$ = 79 nM (37%). For details, see (21).

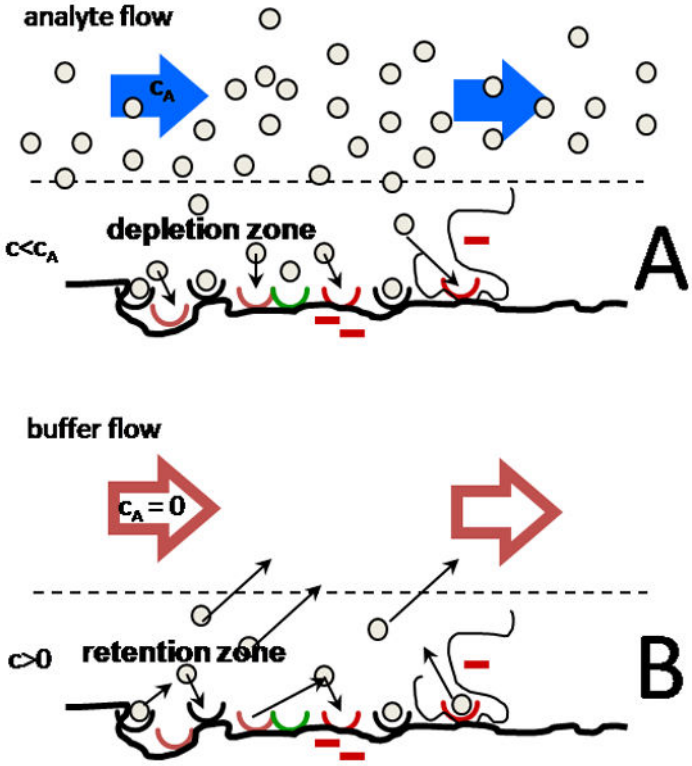

Figure 4.

Cartoon depicting the effect of limited mass transport on the analyte concentration. (A) In the association phase, limited mass transport causes the analyte close to the surface to be bound more quickly than it can be resupplied by the bulk analyte flow. This creates a depletion zone of analyte at the surface, resulting in c (concentration of analyte close to the surface) lower than c_A (concentration of analyte in the bulk). (B) In the dissociation phase, limited mass transport leads to the retention of analyte close to the surface, whereby analyte rebinding to empty surface sites occurs before it can migrate to the bulk flow.

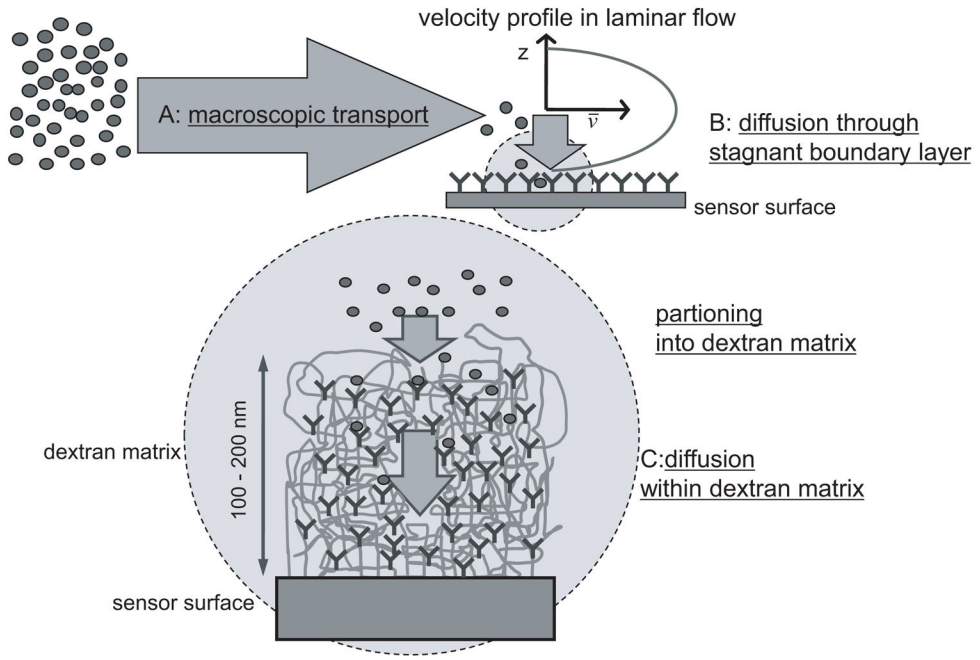

Figure 5.

Schematics depicting the different possible physical origin of mass transport limitation (2). (A) The first, macroscopic step is the transport is through the microfluidic system, and is dependent on the bulk flow rate. (B) The diffusion through the non-stirred boundary layer in laminar flow depends on the bulk flow rate, flow cell geometry, and the diffusion coefficient of the analyte in the bulk solution. If a polymer support, such as the common dextran matrix, is applied, the analyte is partitioning into this matrix. This depends on the size and chemical properties of analyte and polymer matrix. (This step is not a transport step *per se*, but reduces the analyte concentrations and concentration gradients in the matrix, leading to lower transport.) (C) The diffusion through the immobilization matrix depends on the size and charge of the analyte, thickness and density of the dextran matrix, the diffusion coefficient of the reactant in polymer solution and close to surfaces, the spatial distribution of surface binding sites, and on non-specific binding properties.

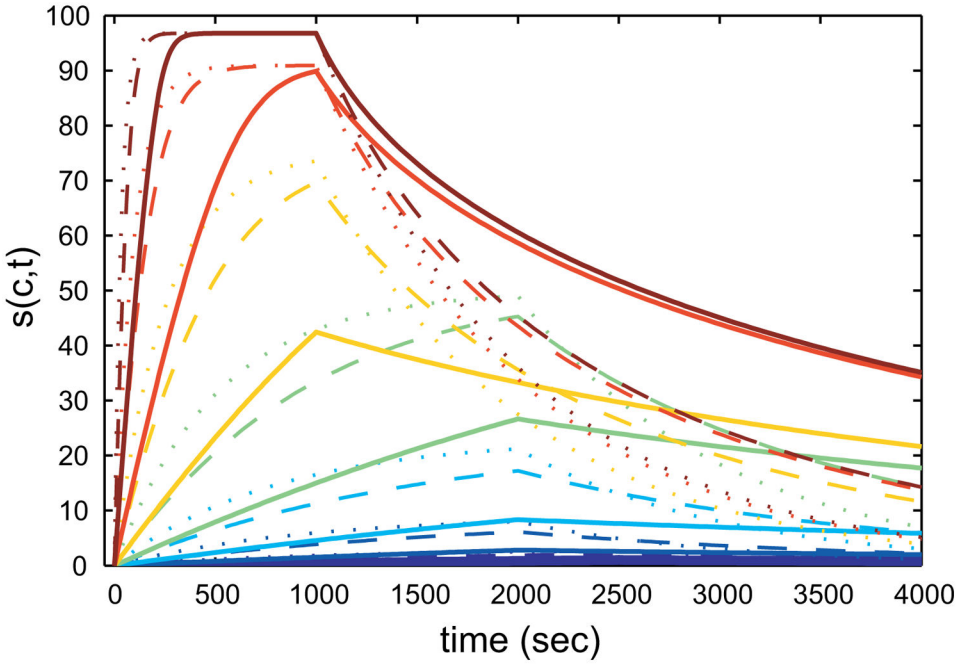

Figure 6.

The effect of limited mass transport on the surface binding kinetics. Mass transport limitation is gradually added to the same theoretical model system as shown in Figure 1: log10(k_{tr}) = 8.48 (dotted lines), log10(k_{tr}) = 7.0 (dashed lines) and log10(k_{tr}) = 6.30 (solid lines). With increasing mass transport limitation (lower transport rate constant k_{tr}), both the association and dissociation phases exhibit slower kinetics. In the association phase, due to the local depletion zone at the surface, slower and more convex binding progress curves are expected. In the dissociation phase, when the rate of dissociation is higher than the transport rate, a non-vanishing concentration of analyte in the vicinity of the sensor surface allows rebinding to empty surface sites. The retention effect results in a slower overall dissociation from the surface and to apparent biphasic decays, in particular when the dissociation is started from close to saturation.

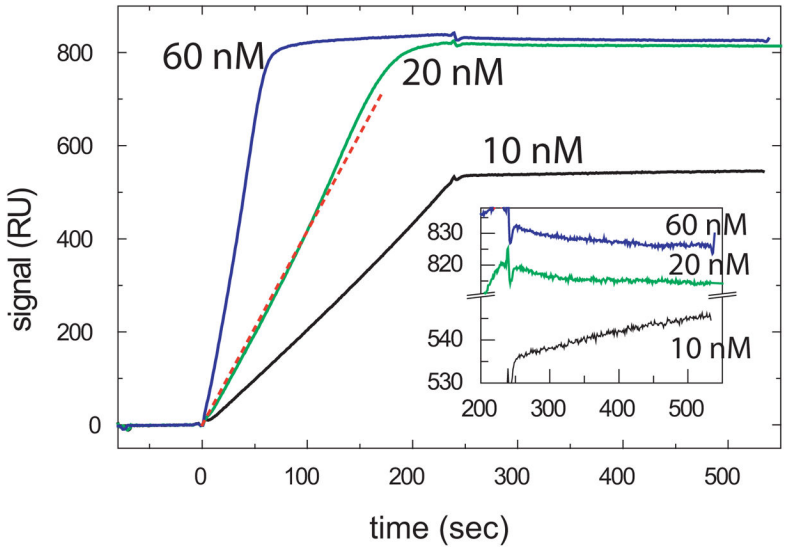

Figure 7.

Illustration of spatial concentration gradients in the sensing volume during mass transportation limitation influencing the surface binding kinetics by creating characteristic, counter-intuitive artifacts (13). HyHel-10 mAb is immobilized to a long-chain carboxymethyl dextran matrix (CM5 chip), and binding of 10 nM, 20 nM, and 60 nM soluble antigen (hen egg lysozyme) is observed at a flow rate of 5 μl/min. To highlight the sigmoid-shaped binding curve with increasing slope that arises when a moving front of saturation enters more sensitive regions, a straight (red dotted line) line is plotted for comparison. The inset shows the dissociation traces after incomplete association in enlarged scale. The increasing signal in the dissociation following the application of the 10 nM sample stems from the slow decay of concentration gradients within the inhomogeneous sensing volume.

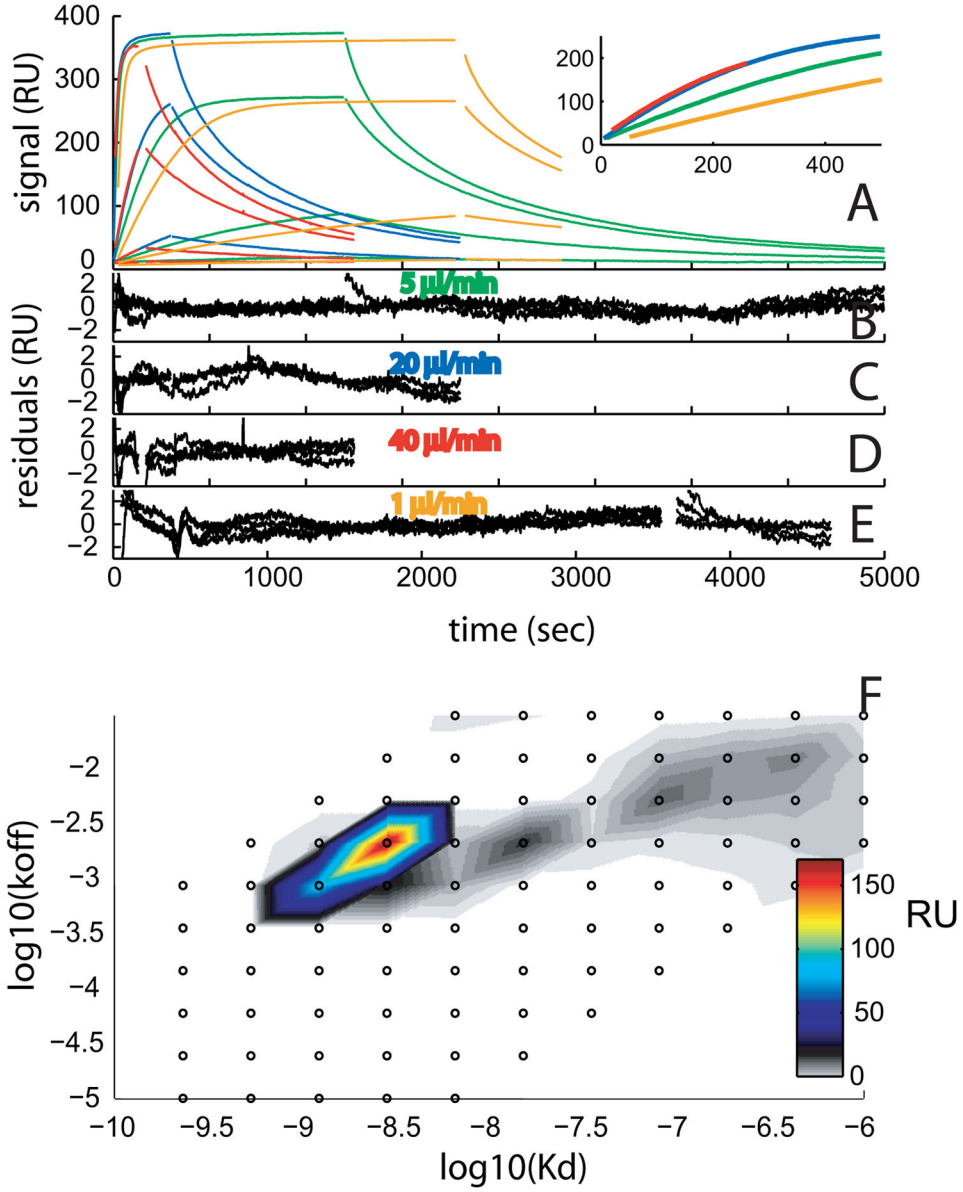

Figure 8.

The effect of flow rate on the surface binding kinetics for mass transport limited binding (13). Shown are surface binding data acquired from the same surface at flow rates of 1, 5, 20, and 40 µl/min, and the global fit with a model for transport-influenced binding to a distribution of surface sites allowing for different transport rate constants at the different flow rates. (A) Experimental data at 1 (orange), 5 (green), 20 (blue), and 40 (red) µl/min for analyte concentrations of 0.1, 1, 10, and 100 nM (no 0.1 nM data available at 20 µl/min). The inset expands the initial association data at an analyte concentration of 10 nM for all flow rates. The results of the global fit are at 5 µl/min: log10(k_{tr}) = 7.91 with an rmsd of 0.53 RU (B), at 20 µl/min: log10(k_{tr}) = 8.18 with an rmsd of 0.79 RU (C), at 40 µl/min: log10(k_{tr}) = 8.21 with an rmsd of 0.66 RU (D). (E) Given the distribution from the fit of the three high flow rates, we applied the distribution as a constant prior knowledge to the data at

1 μl/min, here optimizing solely the transport rate constant, resulting in log10(k_{tr}) = 7.62 with an rmsd of 0.74 RU. (F) Best-fit distribution from the global fit of all data.

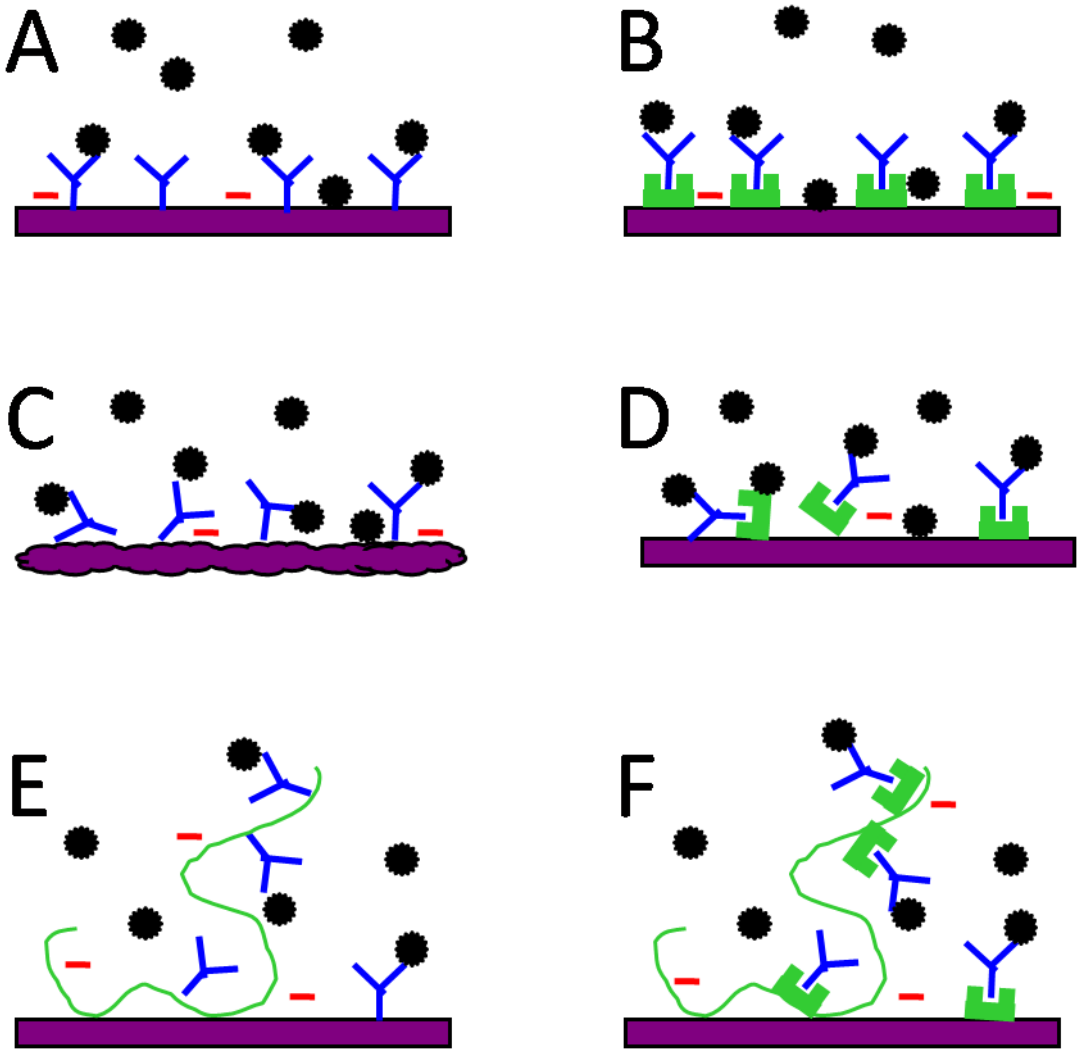

Figure 9.

Cartoon illustrating different sources of heterogeneity of surface binding sites. Filled circles depict the analyte molecules, and 'Y' depicts the macromolecular binding partner to be immobilized and serve as surface binding site. (A) Surface site heterogeneity may occur fundamentally from non-specific binding to the surface. (B) The same is true in the presence of a capturing protein (e.g., an antibody or streptavidin) for the macromolecule of interest. In addition, the capturing molecules may contribute to the available 'non-specific' surface sites. (C) The surface is heterogeneous on a molecular scale both with respect to surface rugosity, as well as surface charges and local pH. (D) The same is true for a capturing protein, which itself may not be oriented uniformly and expose the analyte to different microenvironments. (E) If a polymeric immobilization matrix is used, immobilization to different regions can give rise to different extent of steric hindrance, and heterogeneous microenvironment from spatial and chemical non-uniformity of the matrix. (F) The same effects occur when using a capturing protein, possibly exacerbated due to the overall higher degree of functionalization of the immobilization matrix (higher total protein concentration at the surface).

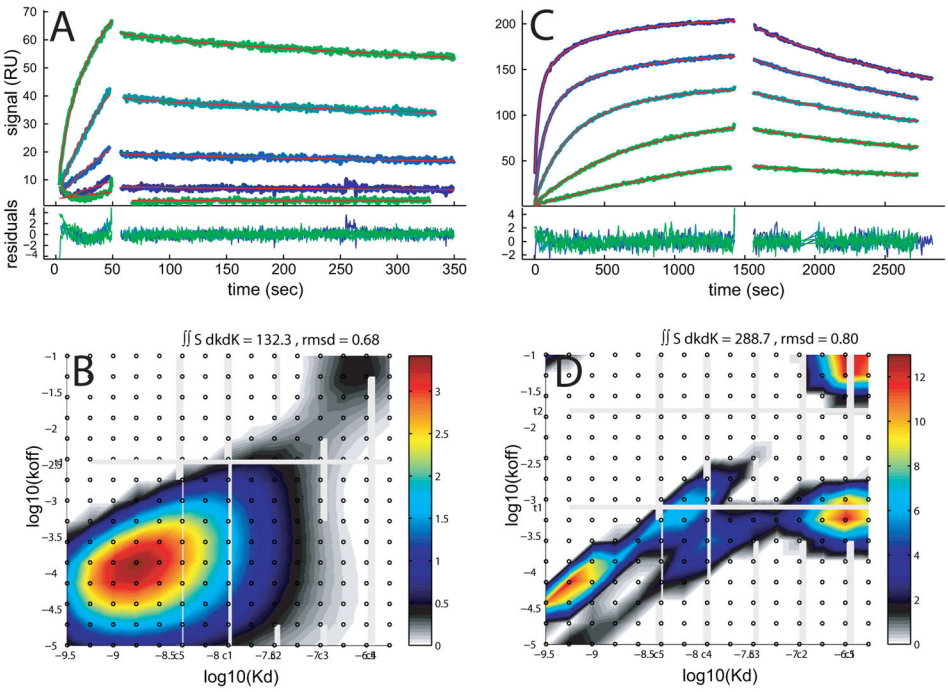

Figure 10.

Comparison of affinity and kinetic rate constant distribution obtained from the same surface from binding experiments with different design. This is the distribution analysis of the same data sets as shown in Figure 3. Excellent fits are achieved for both experimental designs, but the regularization in the distribution analysis exposes different information content. (A) and (B) Arbitrarily truncated data and analysis with short association and dissociation time and a small analyte concentration range. The resulting distribution exhibits only broad features, suggesting not more than the order of magnitude of both the kinetic and affinity binding constants. (C) and (D) Experimental binding data and analysis of longer contact times and larger analyte concentration range. The resulting distribution is very detailed, resolving multiple classes of surface sites. For details, see (53).

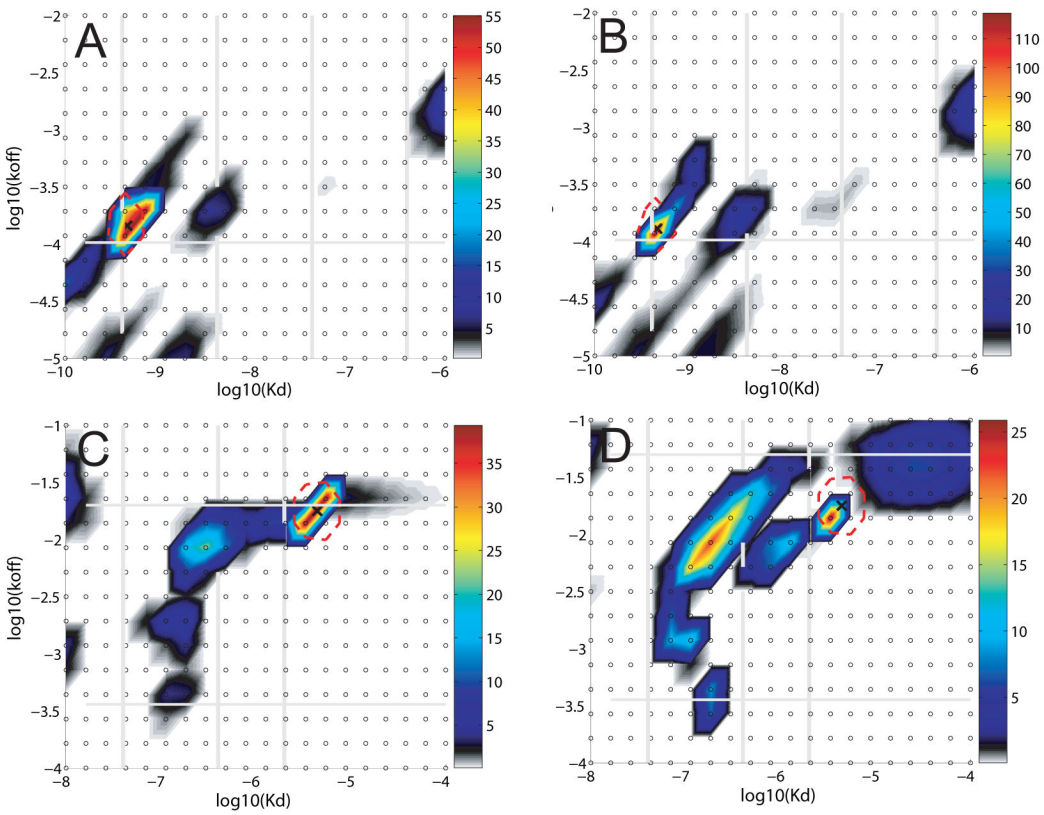

Figure 11.

Example for the affinity and kinetic rate constant distribution measured at surfaces with different immobilization levels. (A) and (B) Binding of a soluble monoclonal Fab to its immobilized antigen protein at a low surface density of 1,400 RU leading to a total binding capacity of ~340 RU (A) and high surface density of 3,800 RU leading to a total binding capacity of ~ 700 RU (B), respectively. For this molecule, the resulting functional surface site distributions are virtually the same, independent of immobilization level. (C) and (D) Binding of another soluble monoclonal Fab to its antigen protein immobilized at low surface density of 920 RU leading to a total binding capacity of 381 RU (C), and immobilized at a higher surface density (1500 RU) leading to a total binding capacity of 464 RU (D). In this case, a significant increase in the fraction of higher affinity sites is observed at the higher density surface. For details, see (19).